JOC The Journal of Organic Chemistry

Article

Neutral Pyrrole Nitrogen Atom as a #- and Mixed n,#-Donor in Hydrogen Bonding

Alexander F. Pozharskii, Valery A. Ozeryanskii, Ekaterina A. Filatova, Olga V. Dyablo, Olga G. Pogosova, Gennady S. Borodkin, Aleksander Filarowski, and Dmitriy V. Steglenko

J. Org. Chem., **Just Accepted Manuscript** • DOI: 10.1021/acs.joc.8b02562 • Publication Date (Web): 21 Dec 2018

Just Accepted

ACS Publications

is published by the American Chemical Society. 1155 Sixteenth Street N.W., Washington, DC 20036

Neutral Pyrrole Nitrogen Atom as a π- and Mixed *n*,π-Donor in Hydrogen Bonding

Alexander F. Pozharskii,*[a] Valery A. Ozeryanskii,[a] Ekaterina A. Filatova,[a] Olga V. Dyablo,[a] Olga G. Pogosova,[a] Gennady S. Borodkin,[b] Aleksander Filarowski,[c] Dmitriy V. Steglenko [ab]

[a] *Department of Organic Chemistry, Southern Federal University, Zorge str. 7, 344090 Rostov-on-Don, Russian Federation. E-mail: apozharskii@sfedu.ru*

[b] *Institute of Physical and Organic Chemistry, Southern Federal University, Stachki Ave. 194/2, 344090 Rostov-on-Don, Russian Federation*

[c] *Faculty of Chemistry, University of Wroclaw, F. Joliot-Curie 14, 50-383 Wroclaw, Poland and Department of Physics, Industrial University of Tyumen, Volodarskogo 38, 625000 Tyumen, Russian Federation*

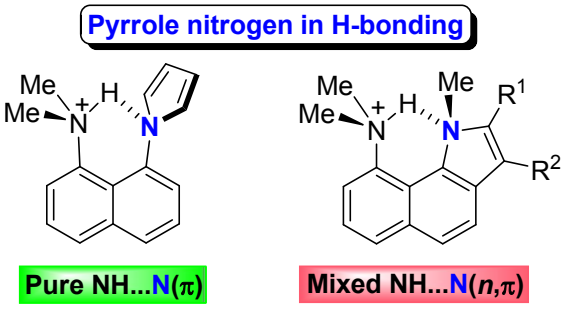

Abstract: 9-Dimethylaminobenzo[*g*]indoles **3**–**6** and 1-dimethylamino-8-(pyrrolyl-1)naphthalene **7** were examined as possible models for establishing the ability of the pyrrole nitrogen atom to participate in the $[NHN]^+$ hydrogen bonding as a proton acceptor. Indoles **3**–**5** (to a lesser extent **6**) form rather stable tetrafluoroborates with the proton mostly located on the NMe_2 group but simultaneously engaged in the formation of charged intramolecular $[NHN]^+$ hydrogen bond (IHB) with the pyrrole N atom. The theoretically estimated energies of IHB in salts $\mathbf{3H^+BF_4^-}$–$\mathbf{6H^+BF_4^-}$ vary between 7.0–10.7 and 6.2–7.0 kcal mol^{-1} in vapor and MeCN, respectively. The pyrrole N atom undergoes a perceptible pyramidalization but still remains involved into the 6π-electron aromatic system, suggesting that the hydrogen bonding in salts $\mathbf{3H^+BF_4^-}$–$\mathbf{6H^+BF_4^-}$ represents a previously unknown mixed NH…N(*n*,π) interaction. Despite the favorable orientation of the N–H bond and the pyrrole ring in salt $\mathbf{7H^+BF_4^-}$, no signs of NH…N(*n*) bonding in it were noticed and the existing interaction was classified as pure NH…N(π). The results obtained may be useful in studies of secondary protein structures, especially those α-helix sections which contain tryptophan residues.

Introduction

For a long time it was believed that the secondary structure of normal natural proteins, which is a right-handed α-helix, is maintained exclusively by multiple NH···O=C hydrogen bonds between the amino

acid residues within one coil of the helix.[1] Similar interactions of more remote helix sites as well as different protein subunits are responsible for the tertiary and quaternary protein structures. However, over time, it came to be understood that such a picture is greatly simplified and many other non-covalent forces are involved in the formation of the spiral structure, such as salt bridges, hydrophobic forces or XH...π binding (X = N, O, S) (reviews[2–4]). Thus, diffraction studies of thousands of protein molecules have shown that the share of such interactions reaches 15% of their total number. As π-donors, aromatic cores of phenylalanine, tyrosine and tryptophan participate in them with the 1 : 1.5 : 5 relative proportion.[2a] The higher activity of the latter is ascribed to the larger electron donor ability of the more expanded indole π-system. X-ray data have disclosed that the X–H…π bonding for tryptophan residues is equally realized via the benzene and pyrrole ring. At the same time, various quantum-chemical calculations of model systems, for example 1-methylindole–H_2O[5a] and 1-methylpyrrole–alkanols[5b] unequivocally give preference to the pyrrole moiety. Normally, the uncharged X–H…π bonds are considered to be rather soft and weak (< 4 kcal mol^{-1})[2] and directed either toward the ring midpoint or the carbon atoms. X-Ray crystal structures for parent pyrrole **1**[6a] (see also ref.[6b]) and 1-phenyl-1-(1H-pyrrole-1-yl)ethanol **2**[7] can serve as typical illustrations. The NH…C_β and OH…C_α distances in these dimeric units are equal to 2.57 and 2.52 Å, respectively (for comparison, the OH…N distance in **2** is of 2.95 Å). This is not surprising since the pyrrole nitrogen atom being a π-electron donor gains partial positive π-charge while the ring carbon atoms receive negative π-charges, which are larger in β-positions.[8]

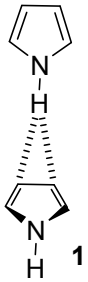

1

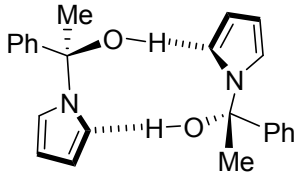

2

To our knowledge, until now there were no reports on the X–H...N(π) or X–H...N(*n*) hydrogen bonding centered on neutral pyrrole nitrogen atom.[9–14] This raises the question: are there any circumstances under which such kinds of binding might be favorable? To answer it, in the present work a possibility of the formation of intramolecular hydrogen bonds (IHB) in protic salts of 1-methyl-9-dimethylaminobenzo[*g*]indoles **3**–**6** and 1-dimethylamino-8-(pyrrolyl-1)naphthalene **7** was studied (Scheme 1). Our choice was based on the following reasoning. First, in view of the importance of the so-called "proximity effect", *peri*-disubstituted naphthalene derivatives for a long time attract deep attention as convenient models for studying various nonconventional interactions.[15] One of the most

striking examples is the observation by Lectka and his group[16] that IHB in the protic salt of *N*-(2-fluorobenzoyl)-*N*,*N*'*N*'-trimethyl-1,8-diaminonaphthalene **8H**$^+$ (Scheme 2) is realized via the amide nitrogen atom, not the carbonyl group, as it normally occurs in amides (see above). Secondly, a comparison of compounds **3H**$^+$**BF**$_4^-$**–6H**$^+$**BF**$_4^-$ and **7H**$^+$**BF**$_4^-$ looks rather intriguing since the pyrrole N atom in the former is positioned in a way excluding competition from the ring carbon atoms while it can not be said about **7H**$^+$**BF**$_4^-$ due to relative flexibility of the 8-pyrrolyl substituent.

Scheme 1. 1-Methyl-9-dimethylaminobenzo[*g*]indoles and 1-Dimethylamino-8-(pyrrolyl-1)naphthalene along with Their Tetrafluoroborates

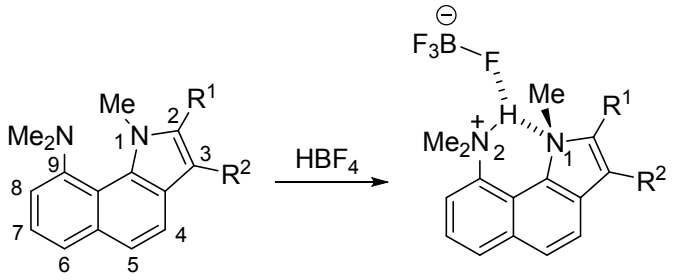

3 (R^1 = R^2 = H) **3H**$^+$**BF**$_4^-$ (R^1 = R^2 = H)
4 (R^1 = 4-MeC_6H_4, R^2 = Me) **4H**$^+$**BF**$_4^-$ (R^1 = 4-MeC_6H_4, R^2 = Me)
5 (R^1 = 4-$O_2NC_6H_4$, R^2 = Me) **5H**$^+$**BF**$_4^-$ (R^1 = 4-$O_2NC_6H_4$, R^2 = Me)
6 (R^1 = H, R^2 = CF_3) **6H**$^+$**BF**$_4^-$ (R^1 = H, R^2 = CF_3)

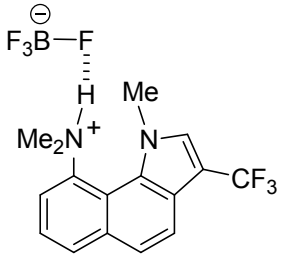

6H$^+$**BF**$_4^-$ **(a)**

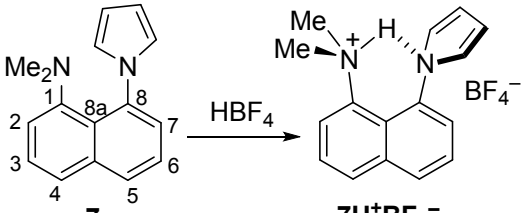

7 **7H**$^+$**BF**$_4^-$

Scheme 2. Some Auxiliary Compounds Mentioned or Studied in This Work

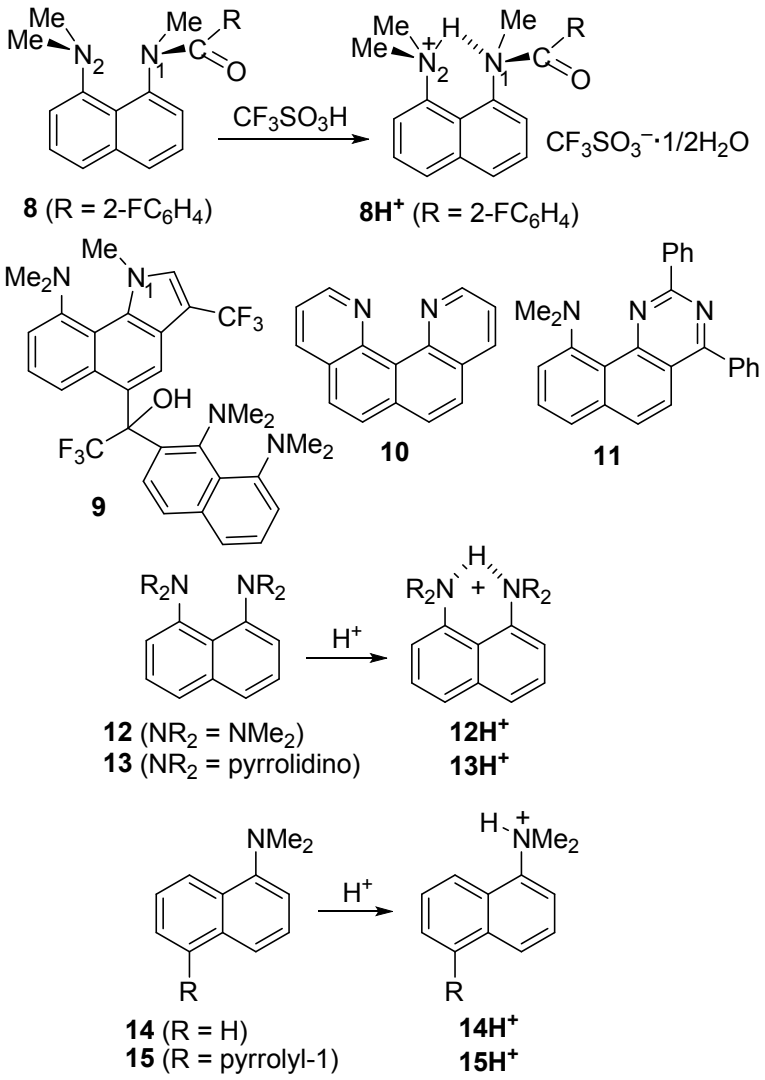

Results and Discussion

Synthesis

The required protic salts $\mathbf{3H^+BF_4^-}$–$\mathbf{6H^+BF_4^-}$ were obtained on treatment of recently described benzo[*g*]indoles **3**–**6**[17] with HBF_4 (see Experimental Section). Previously unknown 1-dimethylamino-8-(pyrrolyl-1)naphthalene (**7**) was synthesized by methylation of amine **16**[18] with dimethylsulfate in the presence of Na_2CO_3 (Scheme 3). This method gave also some amount of monomethylated product **17**. An attempt to synthesize **7** by reacting 1-dimethylamino-8-aminonaphthalene with 2,5-dimethoxytetrahydrofuran in acetic acid failed. At the same time, isomeric to **7** compound **15** (Scheme 2) was easily obtained by this way from 1-dimethylamino-5-aminonaphthalene (see Experimental Section).

Scheme 3. Synthesis of 1-Dimethylamino-8-(pyrrolyl-1)naphthalene (**7**)

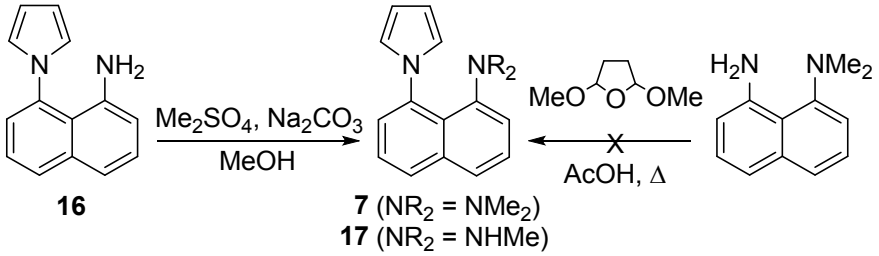

16 **7** (NR_2 = NMe_2)
17 (NR_2 = NHMe)

Protonated Benzo[*g*]indoles

We were managed to grow crystals of salts **3H$^+$BF$_4^-$–5H$^+$BF$_4^-$** from anhydrous acetonitrile and performed their X-ray investigation (ESI, pp. S3–S5). Salt **6H$^+$BF$_4^-$** with CF_3 group in the pyrrole ring due to its caramel-like character and tendency to deprotonation could not be structurally examined. The molecular structures of salts **3H$^+$BF$_4^-$–5H$^+$BF$_4^-$** along with the key geometrical parameters are shown in Figure 1 and Table 1. For comparison, those also include data for bases **4** and **5**, Lectka's amide **8** and its salt **8H$^+$CF$_3$SO$_3^-$**, which is important because the amide N atom in **8**, similar to pyrrole counterparts **3**–**5** donates two electrons into the π-system.

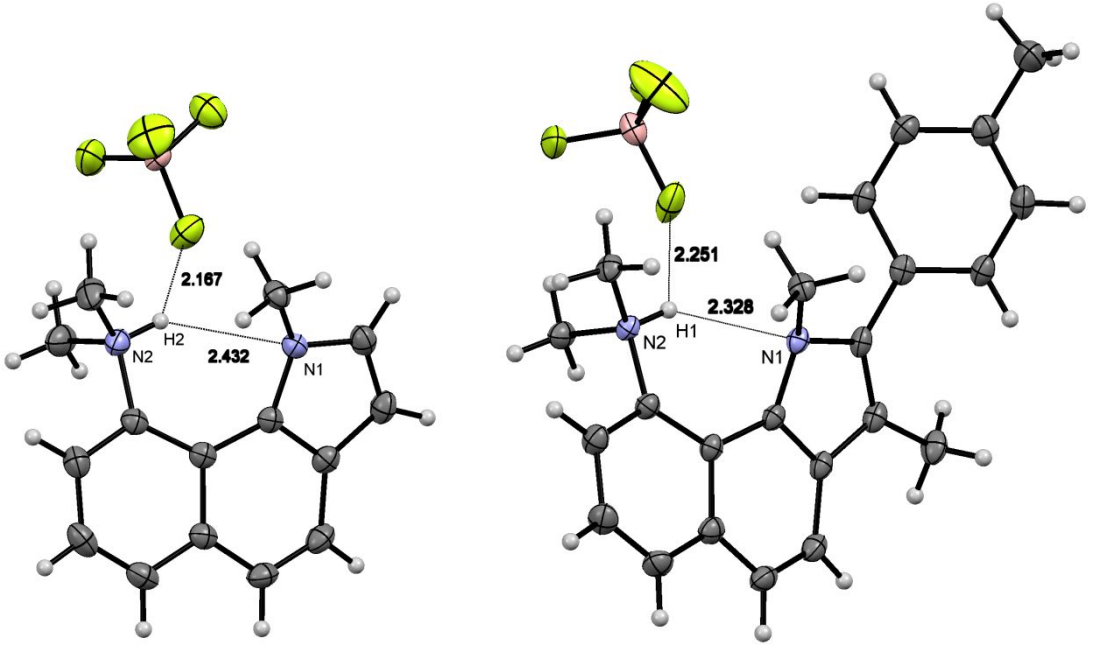

3·HBF$_4$ **4·HBF$_4$**

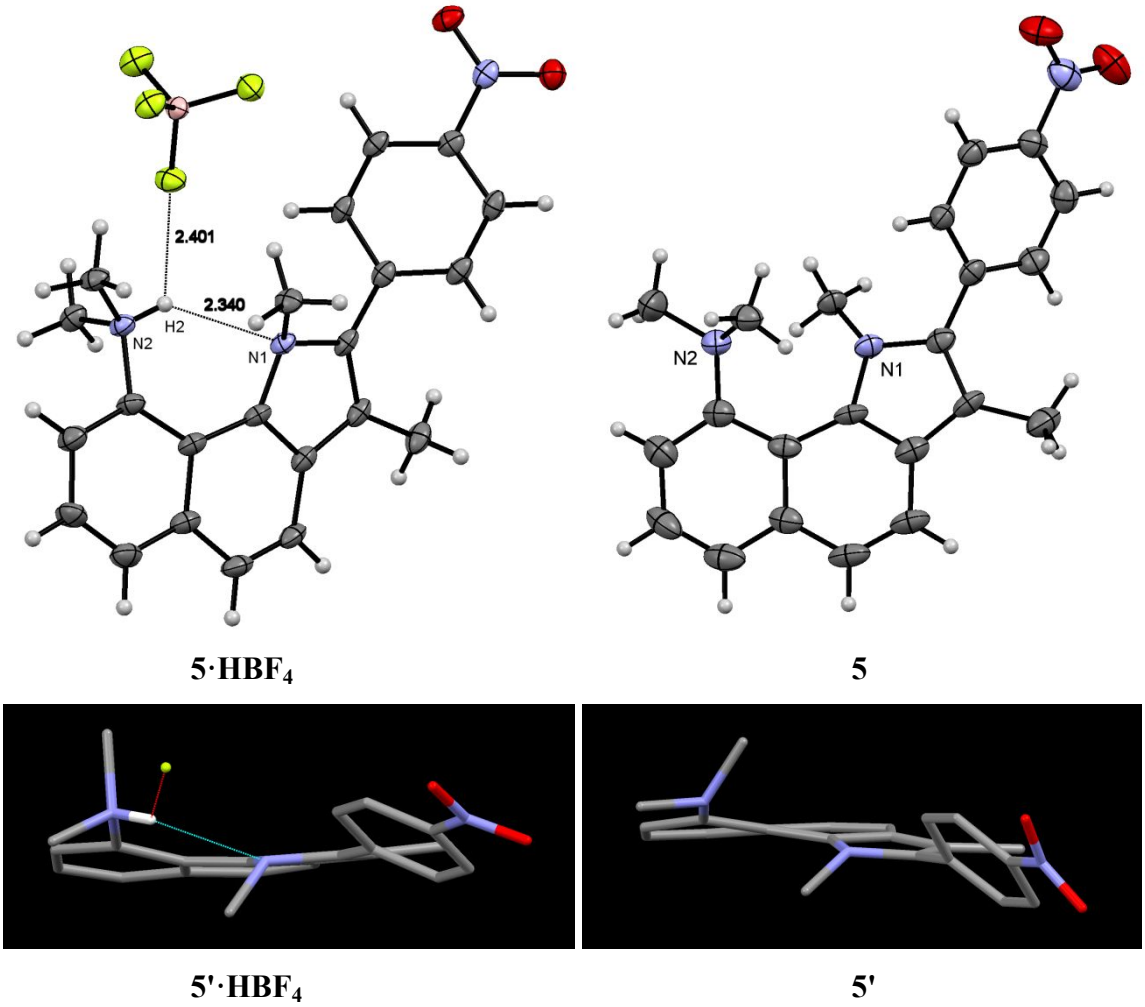

5·HBF$_4$ **5**

5'·HBF$_4$ **5'**

Figure 1. Molecular structures of tetrafluoroborates **3H$^+$BF$_4^-$–5H$^+$BF$_4^-$** and base **5** (*P* = 50%, 120 K, close NH proton–anion and NH proton–pyrrole nitrogen contacts are also given, Å). Two bottom pictures are the view of salt **5·HBF$_4$** and base **5** along the naphthalene ring plane with the *peri*-substituents directed to the viewer; the small yellow-green ball in picture **5'·HBF$_4$** denotes the nearest fluorine atom of the counter-ion.

Table 1. Selected X-ray Diffraction Parameters for Salts **3H$^+$BF$_4^-$–5H$^+$BF$_4^-$**, **8H$^+$CF$_3$SO$_3^-$** and Bases **4**, **5** and **8**

Compd.	Bond lengths and distances, Å				Angles (°) and out-of-plane deviations, Å				Ref.
	N(2)–H	N(1)…H	N(1)…N(2)	H…F	NHN	ΣN(1)	ΣN(2)	ΔMe[a]	
3H$^+$BF$_4^-$	0.91	2.43	3.175	2.17	139	353.4	334.2	0.597	[b]
4H$^+$BF$_4^-$	0.90	2.33	3.074	2.25	140	345.6	334.3	0.843	[b]
5H$^+$BF$_4^-$	0.89	2.34	3.046	2.40	136	342.9	334.2	0.943	[b]
4	–	–	3.051	–	–	354.0	341.8	0.562	17a
5	–	–	3.016	–	–	351.7	347.3	0.676	17b

8H$^+$	0.88	2.17	2.869	–	136	349.3	334.2	–	16
$CF_3SO_3^-$^{c}	0.86	2.21	2.898	–	136	350.4	334.6	–	
8	–	–	2.876	–	–	359.9	339.7	–	16

[a] Deviation of the *N*(1)-methyl group carbon atom from the average pyrrole ring plane. [b] This work. [c] Data for two independent cations are given.

Before discussing the data obtained, it is reasonable to ask a question: which of them could serve as the most decisive argument in favor of the NHN hydrogen bonding? Obviously, such a parameter is the pyramidalization of the pyrrole N atom that increases the stereo orientation of the unshared electron pair orbital towards the proton of the Me_2NH^+ group (see review[19] and ref.[20] for modern view on the related hybridization phenomena). In its turn, the degree of the pyramidalization can be expressed via the sum of the valence angles at the nitrogen atom, ΣN; or alternatively, via the deviation of the pyrrole NMe group from the average heterocyclic plane, ΔMe. For example, in cations of proton sponges **12H**$^+$ and **13H**$^+$ having especially strong IHB with the energy, E_{HB}, estimated near 20 kcal mol^{-1},[21] the ΣN value varies between 336–339°, which is 8–12° less than in the corresponding bases.[22,23] For amide cation **8H**$^+$, the pyramidalization is practically the same (ΔΣN = 10°) and for cations **4H**$^+$ and **5H**$^+$ the ΔΣN's are 8.4 and 8.6°, respectively. These values along with the ΔMe parameters (Table 1) clearly indicate the formation of IHB between the NH group and the pyrrole nitrogen atom in the solid tetrafluoroborates **4H**$^+$**BF**$_4^-$ and **5H**$^+$**BF**$_4^-$. It is noteworthy, that partial pyramidalization exists already in bases **4** and **5** (ΔMe = 0.562 and 0.676 Å, respectively). We attribute this to the steric pressure that the 2-aryl- and partly the 9-NMe_2 substituents exert on the pyrrole NMe group. Yet, as it is seen, the transition to cations **4H**$^+$ and **5H**$^+$ results in considerable extra pyramidalization and is accompanied by a decrease in the rotation angle of the 2-aryl ring relatively the pyrrole cycle (ESI, Table S5).

The structure of cation **3H**$^+$ considerably differ from that of **4H**$^+$and **5H**$^+$. Thus, the N(1) atom in **3H**$^+$**BF**$_4^-$ is more flat [ΣN(1) = 353.4°] as compared with **4H**$^+$**BF**$_4^-$ and **5H**$^+$**BF**$_4^-$ (345.6° and 342.9°) and the deviation of pyrrolic NMe group for **3H**$^+$ is also smaller: ΔMe = 0.597 against 0.843 and 0.943 Å for **4H**$^+$ and **5H**$^+$, respectively (see also estimation of valent orbital contribution for pyrrole N atoms in compounds under study, ESI, p. S100). We think that due to the absence of 2-aryl substituent in **3** its N(1) atom is more involved into the aromatic π-system and therefore extra energy is needed to form the NHN bond in **3H**$^+$.[24,25]

On the whole, the IHBs in the solid salts **3H**$^+$**BF**$_4^-$**–5H**$^+$**BF**$_4^-$ are strongly asymmetric with the NH proton mostly located on the 9-NMe_2 group and with the N(1)…N(2) distance in a range of 3.05–3.17 Å. Though this interval greatly exceeds that in a vast majority of proton sponge cations (2.55–2.60 Å)[22]

it is well below 3.2–3.8 Å what is commonly considered as the typical length for the X–H…π hydrogen bonds in proteins.[2] A rather wide cleft between the nitrogen atoms in **3H$^+$BF$_4^-$–5H$^+$BF$_4^-$** along with a quite sharp NHN angle (136–140°) provokes close proximity of the NH proton and the nearest fluorine atom of the BF_4^- anion with the inverse proportion between the H…F and N…N distances (Table 1). Actually, in the solid salts **3H$^+$BF$_4^-$–5H$^+$BF$_4^-$** we deal with the bifurcated hydrogen bonds and that is why benzo[*g*]indoles **3**–**5** stay structurally much closer to the kinetically active pseudo-proton sponges like **10** or hybrid sponges like **11**[26] rather than to the genuine proton sponges **12** and **13** (Scheme 2).[27]

Another important point, which was revealed during the diffraction studies of salts **3H$^+$BF$_4^-$–5H$^+$BF$_4^-$**, concerns a mode of changing N…N distance on protonation. Usually, in proton sponges and their –N=/–N= and Me_2N/–N= counterparts a transition to the protonated form is accompanied by a considerable contraction of the N…N distance (Figure 2a–c, ΔNN parameter) due to the strain relief at the formation of strong IHB. In contrast, such transition from **3–5** to cations **3H$^+$**–**5H$^+$** leads to slight elongation of the N…N parameter (Figure 2d). Apparently, the presence of both the NH proton and the pyrrole NMe group in the internitrogen space of **3H$^+$BF$_4^-$–5H$^+$BF$_4^-$** hampers the formation of more effective NHN bond (Figure 2d). This conclusion is supported by the analysis of the naphthalene ring deformation (twisting parameter) in the compounds under consideration (ESI, p. S99). Similar behavior was previously noticed for some other proton sponge-like compounds[21,28] and what is especially indicative for Lectka's amide **8**.[16]

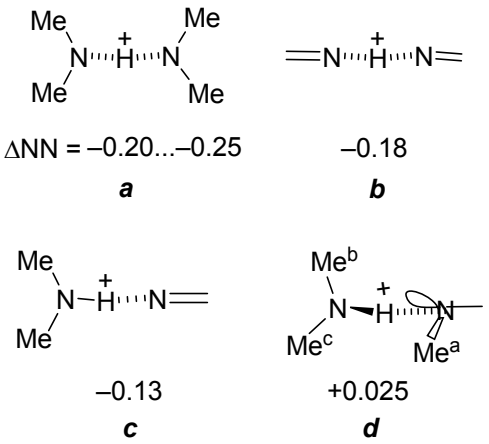

Figure 2. Schematic representation of IHB geometry and typical changes of the average N…N parameter (ΔNN) in protonated *peri*-disubstituted naphthalenes relatively to the corresponding bases: ***a*** – classical proton sponge **14H$^+$**; ***b*** – symmetrical pseudo proton sponge of type **12H$^+$**; ***c*** – hybrid base **13H$^+$**; ***d*** – 9-dimethylamino-1-methylbenzo[*g*]indoles **3H$^+$BF$_4^-$–5H$^+$BF$_4^-$**.

To elucidate structure of salts **3H$^+$BF$_4^-$–6H$^+$BF$_4^-$** in solution, their ^{1}H, ^{13}C and ^{15}N NMR spectra were recorded in CD_3CN together with those of the corresponding bases (ESI, Figures S1–S11). The chemical shift values for the NH, NMe_2 and NMe groups are depicted in Table 2. Thus, in the spectrum

of **6·HBF$_4$**, the NH proton owing to the fast exchange with water admixture manifests itself at δ 4.65 ppm what testifies an absence of IHB in cation **6H$^+$** in solution due to the electron-accepting CF_3 group [see structure **6H$^+$BF$_4^-$(a)**, Scheme 1]. Unlike **6·HBF$_4$**, the NH proton in salts **3·HBF$_4$**–**5·HBF$_4$** under similar conditions does not undergo visible exchange in the NMR time scale and resonates at δ 8.3–8.4 ppm as a markedly broaden signal (Table 2, see also ESI, Figures S1, S4). Such high field chemical shifts contrasting with those in the ^{1}H NMR spectra of cations **10H$^+$**–**13H$^+$** (δ_{NH} = 17–20 ppm)[22,23,25,27] may result from a relative weakness of IHB in **3·HBF$_4$**–**5·HBF$_4$**. At the same time, it should be recalled (see above) that the NH proton in the latter is significantly deviated from the plane of the aromatic system and thus can be affected by the paramagnetic component of the ring electron current. This helps to understand why the δ_{NH} values for amide cation **8H$^+$** (11 ppm in MeCN)[16] and even for dimethyl(naphthyl-1)ammonium perchlorate **14·HClO$_4$** (this work: 9.47 in MeCN; 10.45 ppm in $CDCl_3$) and 1-dimethyl(5-pyrrolylnaphthyl-1)ammonium picrate **15·PicOH** (this work: 13.2 ppm, $CDCl_3$) are larger than those for **3·HBF$_4$**–**5·HBF$_4$**.

Table 2. Selected Chemical Shift Values (δ, ppm, CD_3CN, 30 °C) for Benzo[*g*]indoles **3**–**6** and Their Tetrafluoroborates **3·HBF$_4$**–**6·HBF$_4$**

Compound	^{1}H			^{13}C		^{15}N	
	NH	NMe_2	NMe	NMe_2	NMe	NMe_2	N_{Het}[a]
3	–	2.65	4.02	42.7	39.4	42.9	138.2
4	–	2.76	3.61	42.4	38.5	43.4	128.4
5	–	2.78	3.63	42.5	39.0	43.2	126.8
6[b]	–	2.69	4.06	43.3	40.3	43.4	139.2
3·HBF$_4$	8.28	3.39	3.88	50.1	38.0	[c]	126.6
4·HBF$_4$	8.42	3.49[d]	3.43	50.0	39.1	49.8	117.6
5·HBF$_4$	~8.4[e]	3.52	3.46	50.2	39.3	[c]	[c]
6·HBF$_4$	4.65[f]	3.42	4.00	50.4	38.4	50.4	135.2

[a] Heterocyclic nitrogen. [b] In $CDCl_3$; ref.[25] [c] Reliable signal could not be registered due to dynamics. [d] A doublet with ^3J = 4.61 Hz. [e] This peak partially overlaps with a doublet from 4-$O_2NC_6H_4$ group. [f] Common peak for the NH/H_2O species due to a fast exchange.

The proton chemical shifts of the NMe_2 and pyrrole NMe groups for bases **3**–**6** and tetrafluoroborates **3·HBF$_4$**–**5·HBF$_4$** are also instructive. Commonly, for the proton sponge, a transition from the neutral base to the nearly symmetrical protonated form (**12** → **12H$^+$**) is accompanied by a low-field shift of the NMe_2 peaks (Δδ ~ +0.3 ppm).[22] Unlike this, the protonation of **3**–**6** results in

increasing the chemical shifts by 0.65–0.75 ppm which is twice as large as in **12**. Clearly, this once again evidences preferable localization of the NH proton in **3·HBF$_4$**–**5·HBF$_4$** on the 9-NMe$_2$ group. Notably, that in the spectrum of **4·HBF$_4$**, the signal of the NMe$_2$ group resonates as a doublet with ^3J(NH,NMe) = 4.61 Hz (2.6 Hz for **12H**$^+$);[22] for **3·HBF$_4$** and **5·HBF$_4$** it appears as a broaden singlet likely due to enhanced dynamics. Such dynamics also accounts for the significant signal broadening of the aromatic protons in the spectra of **3·HBF$_4$** and **5·HBF$_4$**.

The behavior of the pyrrole NMe group on protonation of bases **3**–**6** is completely different. In this case the hydrogen signal of the NMe fragment moves relatively the corresponding base to a high-field region (Δδ = –0.14…–0.18 ppm). We assume that this phenomenon results from a larger extent of sp^3-hybridization of the cyclic nitrogen atom in cations **3H**$^+$–**5H**$^+$, which can be treated as another weighty proof for the formation of IHB in salts **3·HBF$_4$**–**5·HBF$_4$**. Nitrogen spectra in general confirm this picture, while carbon spectra are less informative. From all of the above one can conclude that the IHB strength in cations under consideration both in MeCN solution and in the solid changes in the sequence **5H**$^+$ ≈ **4H**$^+$ > **3H**$^+$ > **6H**$^+$.

Finally, we have estimated basicities of benzo[*g*]indoles **3** and **4** by measuring their pK_a values in MeCN solution via competitive NMR monitoring (ESI, p. S104). We proceeded from the fact that, when protonation is accompanied by the formation of chelated cation this commonly results in increasing pK_a, i.e. basicity, relatively a standard base whose cation is not stabilized by IHB. Proton sponge **12** (pK_a = 18.6, MeCN)[29] and 1-dimethylaminonaphthalene **14** (pK_a = 11.3, MeCN)[30] are textbook examples of this pattern. The pK_a values obtained by us for **3** and **4** (12.8 and 13.5, respectively) follow this rule thus leaving no doubts in the existence of weaker but quite pronounce IHB in their cations in solution. We could not measure pK_a for 4-nitrophenyl derivative **5** in MeCN due to solubility restrictions.

Protonated 1-Dimethylamino-8-(pyrrolyl-1)- and 8-phenylnaphthalenes

Regrettably, our attempt to conduct the X-ray diffraction study of salt **7·HBF$_4$** failed.[31] However, in the case of base **7** we were more successful and the results obtained, along with theoretical calculations, turned out to be helpful. Rather strained X-ray structure of **7** (ESI, Figure S37a) closely reminds that of diamine **12**. This includes noticeably twisted naphthalene framework, nitrogen atoms diverging in different sides from the averaged naphthalene ring plane, and the *N*-methyl groups turned away from the internitrogen space. Besides, the pyrrole ring in **7** faces the amine nitrogen free electron pair as if the molecule were already pre-organized to form NH…π or NH…N(*n*) hydrogen bond. To our

satisfaction, the solid structure of **7** was surprisingly close to the calculated one for the gas phase (ESI, Figure S37b, Table S11) what allowed to be treated with confidence in the theoretical characteristics of **7·HBF$_4$** (Figure 3).

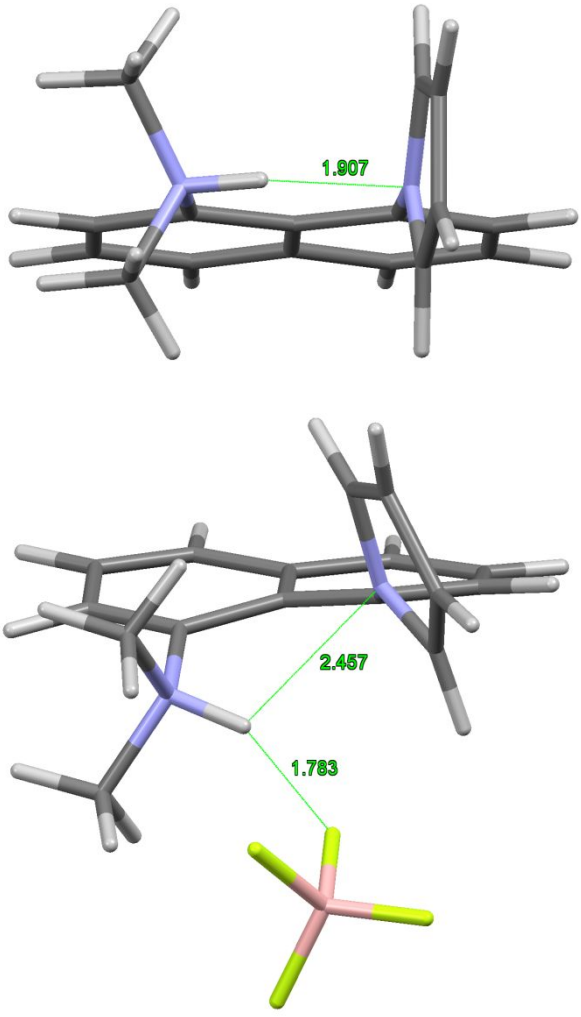

Figure 3. DFT calculated structures of "naked" cation **7H**$^+$ (*a*) and tetrafluoroborate **7·HBF$_4$** (*b*) (in vapor). Both structures are shown with the *peri*-substituents directed to the viewer.

In the "naked" cation **7H**$^+$ (Figure 3a, Table S12) the pyrrole ring is perfectly flat (ΣN_1 = 359.8°) and strictly perpendicular to the naphthalene plane (Θ = 90°). Accordingly, the N–H bond points the pyrrole ring face with the NH proton being closer to the ring N atom (1.907 Å) rather than to C_α (2.324 Å) or to the ring centroid (2.168 Å). In salt **7·HBF$_4$** (Figure 3b, Table S12), the cation structure undergoes significant changes owing to the attractive interaction between the anion BF_4^- and the NH proton. This is evidenced by the very short NH...F distance (1.783 Å against 2.457 Å for NH…N), the increase in the sharpness of the NHN angle (112.1° against 146.6° in **7H**$^+$), the larger asymmetry of the IHB and, particularly, by marked deviation of the proton NH away from the naphthalene ring plane.

Following the last change, the pyrrole ring also rotates to some angle (Θ = 73.1°), as if trying to preserve the interaction with the NH proton. At the same time, the pyrrole N atom in **7·HBF$_4$** remains essentially flat undergoing only subtle pyramidalization (ΣN_1 = 356.8°). From this, one can conclude that in **7·HBF$_4$** we deal with the almost pure NH...N(π) interaction where the pyrrole N atom acts just as a component of the aromatic π-system. Clearly, the closeness of the NH proton in **7·HBF$_4$** to the pyrrole N atom results from the molecular arrangement although a minor contribution of the NH...N(*n*) binding should not be fully rejected.

Such view is generally consisted with ^{1}H NMR spectroscopy. Salt **7·HBF$_4$** was generated directly in the NMR ampoule by adding an equivalent amount of HBF_4 to a solution of **7** in MeCN. In the protic spectrum of **7·HBF$_4$** the signals of all protons are expectedly shifted to a low field relatively the base while keeping unchanged general spectral pattern (ESI, compare Figures S13 and S20). The only exception is the highly broaden NH peak which appears at δ 6.41 ppm, *i.e*. in unusually strong field for the chelated proton (*cf*. with δ ~8.4 and 4.65 ppm for benzo[*g*]indole salts **3·HBF$_4$**–**5·HBF$_4$** and **6·HBF$_4$**, respectively, Table 2). In our opinion, this fact can be attributed both to the influence of the paramagnetic component of the pyrrole ring current in **7·HBF$_4$** and some weakening of IHB due to the considerable bifurcation. Indeed, the δ_{NH} value for molecular complex **15·PicOH** (13.2 ppm) with the ammonium and pyrrole fragments on the opposite sides of the naphthalene core, is much larger than those for **7·HBF$_4$** (ESI, Figures S28 and S38).

In the above context, it seemed rather interesting to perform similar studies for previously unknown 1-dimethylamino-8-phenylnaphthalene (**18**) and its salt **18·HBF$_4$**. This model compound was prepared via standard Suzuki procedure on treatment of 1-bromo-8-acetylaminonaphthalene with phenylboronic acid, followed by hydrolysis, *N*,*N*-dimethylation, and protonation steps (see Experimental Section). The X-ray diffraction study of **18·HBF$_4$** (Figure 4) has revealed the formation of the perfect NH...π hydrogen bond in cation **18H$^+$** and the absence of any bifurcation involving the anion BF_4^-. In the ^{1}H NMR spectrum of the tetrafluoroborate in MeCN, the proton NH appears as a broad signal at δ 8.1 ppm (Figure S34). From this, one can suggest that the NH…π interaction in **18·HBF$_4$** in solution is stronger than in **7·HBF$_4$** and is commensurable with that in benzo[*g*]indole salts **3·HBF$_4$**–**5·HBF$_4$** (see also discussion in the last section).

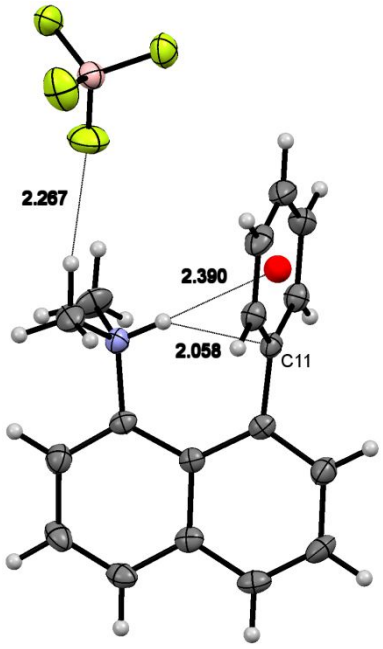

Figure 4. X-ray structure of salt **18·HBF$_4$** (P = 50%, 120 K, close cation–anion and NH proton–phenyl ring contacts are given, Å). Key parameters: N…C_{11} = 2.858 Å, N...H = 0.91 Å, ∠NHC_{11} = 146°, ∠NH…centroid = 173°; Ph rotation angle, Θ = 83.7°.

Hydrogen Bond Energy

In the above discussion, we qualitatively ranged the salts under study for the strength of their IHB, based on the solid X-ray and solution NMR data. To achieve more accurate estimate we then performed the DFT calculations of the IHB energies, E_{HB}, using the B3LYP method with the 6-311++G** basis set. The calculations were conducted both for "naked" cations and tetrafluoroborate salts in the gas phase and acetonitrile solution. Three previously reported approaches were tested for this. The first one known as isodesmic[21] gave the results badly consistent with the experiments (for details see ESI, pp. S100–S102). In contrast, the second approach, which can be called "rotational",[32] turned out to be more realistic. In accordance with it, the E_{HB} values were obtained as a difference between the total energies for the computationally optimized chelated (close) and non-chelated (open) forms (Scheme 4, see also ESI, Table S10).

Scheme 4. Structures with Close and Open IHBs Used for Calculation of E_{HB} Values by "Rotational" Method

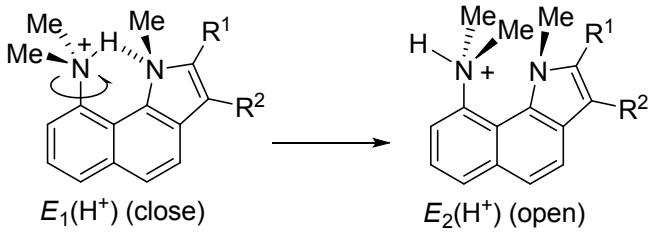

$E_1(H^+)$ (close) $E_2(H^+)$ (open)

3H⁺ ($R^1 = R^2 = H$)
4H⁺ ($R^1 = p$-Tol, $R^2 = Me$)
5H⁺ ($R^1 = p$-$O_2NC_6H_4$, $R^2 = Me$)
6H⁺ ($R^1 = H$, $R^2 = CF_3$)

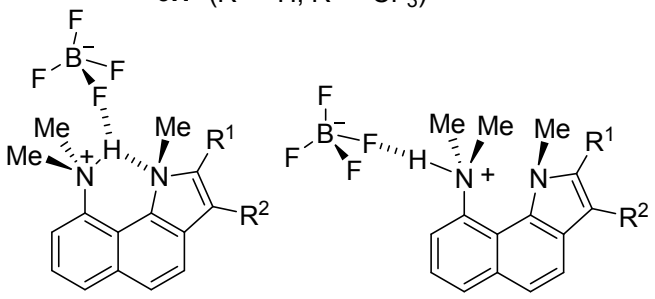

$E_1(HBF_4)$ (close) $E_2(HBF_4)$ (open)

3H⁺BF₄⁻ ($R^1 = R^2 = H$)
4H⁺BF₄⁻ ($R^1 = p$-Tol, $R^2 = Me$)
5H⁺BF₄⁻ ($R^1 = p$-$O_2NC_6H_4$, $R^2 = Me$)
6H⁺BF₄⁻ ($R^1 = H$, $R^2 = CF_3$)

$$E_{HB} = E_1 - E_2$$

Table 3. Calculated Hydrogen Bond Energies, E_{HB}, in "Naked" Cations (B3LYP/6-311++G**)

Cation	Medium	Calculation approach	E_{HB} kcal/mol	E_{HB}(ZPE) kcal/mol
3H⁺	Vapor	Rotational	–10.5	–10.7
3H⁺	MeCN	Rotational	–8.8	–8.8
3H⁺	Vapor	NBO	–7.3	–
4H⁺	Vapor	Rotational	–11.2	–11.4
4H⁺	MeCN	Rotational	–9.4	–9.7
4H⁺	Vapor	NBO	–10.7	–
5H⁺	Vapor	Rotational	–10.9	–11.1
5H⁺	MeCN	Rotational	–9.2	–9.8
5H⁺	Vapor	NBO	–9.2	–
6H⁺	Vapor	Rotational	–10.0	–10.2

6H$^+$	MeCN	Rotational	–8.4	–8.8
7H$^+$	Vapor	Rotational	–13.3	–13.9
7H$^+$	MeCN	Rotational	–11.4	–11.4
18H$^+$	Vapor	Rotational	–13.7	–13.8
18H$^+$	MeCN	Rotational	–11.7	–11.8

Table 4. Calculated Hydrogen Bond Energies, E_{HB}, in Tetrafluoroborates (B3LYP/6-311++G**, "Rotational" Approach)

Salt	Medium	E_{HB} kcal/mol	E_{HB}(ZPE) kcal/mol	Salt	Medium	E_{HB} kcal/mol	E_{HB}(ZPE) kcal/mol
3H$^+$BF$_4^-$	Vapor	–7.1	–7.0	**6H$^+$BF$_4^-$**	Vapor	–7.6	–7.4
3H$^+$BF$_4^-$	MeCN	–6.6	–6.2	**6H$^+$BF$_4^-$**	MeCN	–6.6	–6.5
4H$^+$BF$_4^-$	Vapor	–9.9	–9.6	**7H$^+$BF$_4^-$**	Vapor	–1.9	–1.8
4H$^+$BF$_4^-$	MeCN	–6.9	–6.5	**7H$^+$BF$_4^-$**	MeCN	–6.2	–6.5
5H$^+$BF$_4^-$	Vapor	–11.0	–10.7	**18H$^+$BF$_4^-$**	Vapor	–6.6	–6.2
5H$^+$BF$_4^-$	MeCN	–7.2	–7.0	**18H$^+$BF$_4^-$**	MeCN	–8.6	–8.5

The results obtained (Tables 3 and 4) lead to the following conclusions.

1) The first thing that attracts attention is seemingly inflated E_{HB} values. This can be attributed to two peculiarities of the studied models: participation in the binding of a positively charged proton-donor functionality,[2] Me_2NH^+, and the widely known specifics of *peri*-interactions providing the close proximity of interacting groups and their fairly rigid spatial fixation.[33] Nevertheless, we are not inclined to discount the probability that the E_{HB} values obtained may indeed be somewhat overestimated due to differences in the strain energies, E_{SE}, of the close and open forms shown in Scheme 4. Thus, in case of the benzo[*g*]indole cations, the strain energy in the close form can result from the repulsion of the nearby located NH proton and pyrrolic NMe group. In the open form, such repulsion should be even greater, since it involves already three *N*-methyl groups. Unfortunately, when calculating the E_{HB} values by "rotational" method, it is difficult to obtain a sufficiently accurate correction for the difference between spatial destabilization of the close and open forms since the E_{HB} itself, at such approach, actually consists of two components: hydrogen bonding and strain energies. Yet, we tried to estimate it, at least roughly, by calculating the energies of similar rotational conformers for non-protonated bases **3** and **4** and taking the difference between them: $E_{SE}(\text{base}) = E_1 - E_2$ (Scheme 5). The

E_{SE}(base) values obtained for the gas phase and the acetonitrile solution for **3** and **4** range between 5.8 and 6.7 kcal mol^{-1}. Subtracting them from the E_{HB} given in Table 3, one can get the E_{HB}(corr) values, which lie in the range 3–5 kcal mol^{-1}. However, despite the fact that they look being in harmony with the energies accepted for the NH...π interactions in natural proteins, it is difficult to consider them as realistic because of the neglect of the strain energies in the cations. We then reasoned that a possible way to improve the situation would be to calculate E_{HB} by means of the so-called natural bond orbital method (NBO).[34] The point is that the NBO does not consider two forms, close and open, and involves calculating the electron transfer energy (it is usually designated as $E^{(2)}_{D\rightarrow A}$ interaction) from the *n*-orbital occupied by an unshared electron pair of a donor atom onto the antibonding σ-orbital of the X–H bond (N–H in our case). We tested this method on "naked" cations **3H**$^+$–**5H**$^+$, obtaining the gas-phase hydrogen bond energies for them equal to –7.3, –10.7 and –9.2 kcal mol^{-1}, respectively (Table 3). As it is seen, the course of these changes qualitatively coincides with the X-ray diffraction and NMR spectral data but the E_{HB} themselves are in absolute values smaller than those obtained by the uncorrected (Table 3) "rotational" method by 3.2, 0.5 and 1.7 kcal mol^{-1}, respectively. From this, one can conclude that NBO values adequately reflect the necessary corrections for the strain energies, which should be taken into account when considering the E_{HB} obtained by the "rotational" method. Nevertheless, without having a complete set of NBO data, we left in Table 3 the uncorrected "rotational" values, bearing in mind that their absolute values should be on average 1.5–2 kcal less.

Scheme 5. Estimation of Strain Energy in "Open" Forms of Bases **3** and **4**

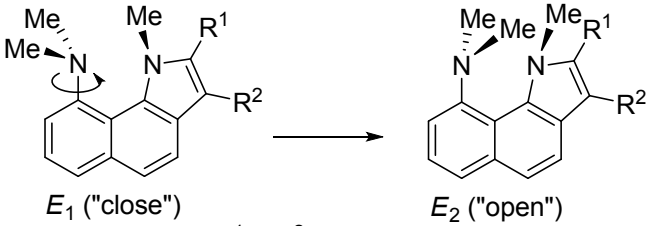

E_1 ("close") E_2 ("open")

3 ($R^1 = R^2 = H$)
4 (R^1 = *p*-Tol, R^2 = Me)

E_{SE}(base) = $E_2 - E_1$

2) The NHN hydrogen bond energies for the "naked" benzo[*g*]indole cations **3H**$^+$–**6H**$^+$ are larger than those for tetrafluoroborates by 3.7, 1.8, 0.4 and 2.8 kcal mol^{-1}, respectively (vapor, ZPE). Obviously, this phenomenon is due to the bifurcation of the hydrogen bond in the case of tetrafluoroborates (see above and below the additional discussion on this topic).

3) In the series of benzo[*g*]indole cations, the IHB strength decreases by 1–2 kcal mol^{-1} upon transition from the gas phase to the acetonitrile solution. This applies to both "naked" cations and tetrafluoroborates.

4) It is known that the hydrogen bond of general form X–H…Y has a predominantly electrostatic nature with a certain contribution of the covalent term.[35] Visually, this can be expressed through the principal possibility of proton transfer (PT) from X to Y: X–H...Y ⇄ X...H–Y. A two-well potential corresponds to such proton motion. The ease of the PT (the height of the barrier) and therefore the strength of the hydrogen bonding increase as the X…Y distance becomes shorter. To date, cations of proton sponges, for example **12H**$^+$ and **13H**$^+$, are recognized as one of the best models for the study of PT due to importance of this question for mechanism of enzyme catalysis.[15c,36] Usually, the barrier height for proton sponges does not exceed 4.5 kcal mol^{-1},[36c] but in case of species with strongly compressed IHB, *e.g.* the cation of 1,8-bis(dimethylamino)-2,7-bis(trimethylsilyl)naphthalene, the barrier drops to 0.7 kcal mol^{-1}.[37]

Importantly, that the very fact of realizing two-well profile can be interpreted in favor of the existence of IHB, whereas both the barrier height and the energy of the PT structure indicate the ease of the proton motion and relative hydrogen bond strength. Taking these circumstances into account, we performed gas phase calculations of PT for "naked" cations **3H**$^+$–**7H**$^+$ (Figure 5). The points on the potential energy curves represent energy changing as the NH proton moves from the 9-NMe_2 group towards the pyrrole nitrogen atom. The results obtained demonstrate that, despite the considerable localization of the proton in **3H**$^+$–**6H**$^+$ onto the NMe_2 group, its transfer to the pyrrole N atom is allowed, since all **3H**$^+$**(PT)**–**6H**$^+$**(PT)** structures lie in the potential minima. Judging from their energy and barrier heights, the benzo[*g*]indole cations are arranged in the following sequence, characterizing the decrease in the NHN strength: **4H**$^+$ > **5H**$^+$ > **3H**$^+$ > **6H**$^+$. As can be seen, this row corresponds exactly to the estimates obtained from other data (see above). In contrast, no minimum has been found for the **7H**$^+$**(PT)** form testifying the absence of the proton transfer, even in spite of the shorter inter-nitrogen distance in **7H**$^+$ (2.82 Å) than in **3H**$^+$ and **4H**$^+$ (2.89 and 2.95 Å, respectively). We assume that this stems from the higher aromaticity of the pyrrole ring in **7** as compared with that in benzo[*g*]indoles **3**–**6**; as a consequence, pyrrolium cation **7H**$^+$**(PT)** differs by smaller stability. On the other hand, simple calculations demonstrates that the losses in the aromatic resonance energy associated with the pyramidalization of the pyrrole nitrogen atom in cations **3H**$^+$–**5H**$^+$ are rather insignificant and are compensated by the energy gain from the intramolecular NHN binding (ESI, pp. S102–S103).

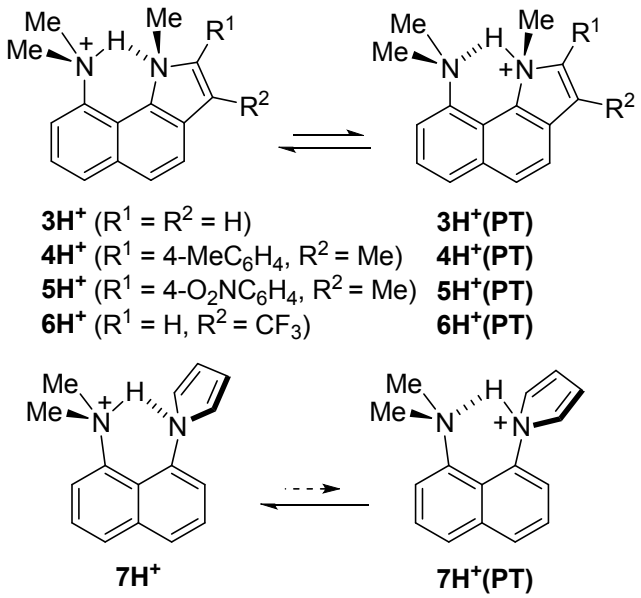

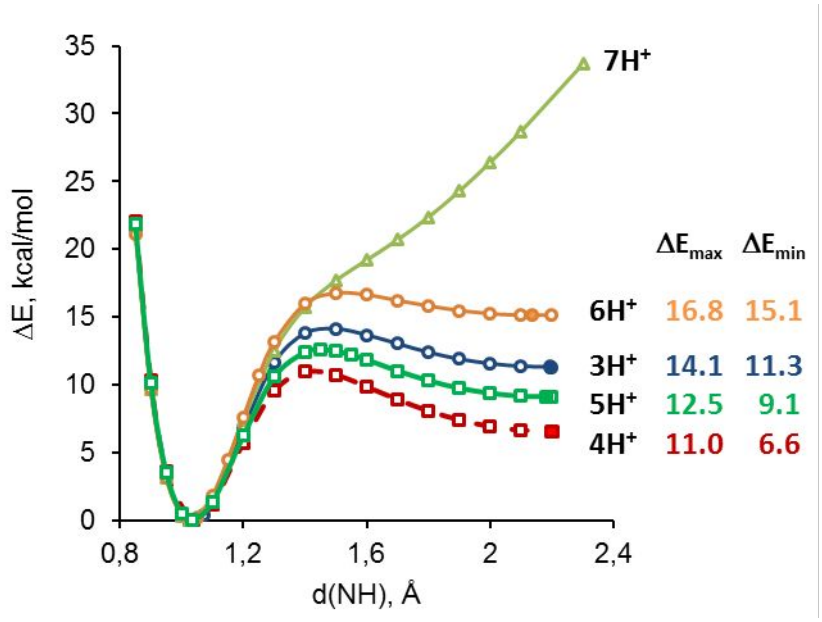

Figure 5. Calculated [B3LYP/6-311++G(d,p)] potential energy curves for the gas phase proton transfer in cations **3H**$^+$–**7H**$^+$ [d(NH) – distance between the proton and the nitrogen atom of NMe_2 group].

5) In accordance with theoretical calculations, the "naked" cations both in vapor and MeCN form the identical sequences in the order of decreasing the IHB strength. As can be seen, the relative position of the benzo[*g*]indole cations is generally in accord with that observed in experimental studies. The priority of cations **7H**$^+$ and **18H**$^+$ can be explained by the flexibility of the pyrrolyl and phenyl rings providing the most favorable orientation for pure NH…π interaction.

"Naked" cations:

Gas phase: **18H**$^+$ ≈ **7H**$^+$ > **4H**$^+$ > **5H**$^+$ > **3H**$^+$ > **6H**$^+$

MeCN solution: **18H**$^+$ > **7H**$^+$ > **4H**$^+$ ≈ **5H**$^+$ > **3H**$^+$ ≈ **6H**$^+$

The situation with tetrafluoroborates is not so unambiguous. In MeCN media, salt **18H**$^+$**BF**$_4^-$ remains first but **7H**$^+$**BF**$_4^-$ moves to the end of the row. The permutations are even more dramatic in the gas phase where IHB's in **7H**$^+$**BF**$_4^-$ and **18H**$^+$**BF**$_4^-$ become the weakest dropping to –1.8 and –6.2 kcal mol^{-1} (ZPE correction), respectively. At the same time, relative arrangement of the benzo[*g*]indole tetrafluoroborates is practically unchanged.

Tetrafluoroborate salts:

Gas phase: **5H**$^+$ > **4H**$^+$ > **6H**$^+$ > **3H**$^+$ > **18H**$^+$ >> **7H**$^+$

MeCN solution: **18H**$^+$ > **5H**$^+$ > **4H**$^+$ ≈ **6H**$^+$ ≈ **7H**$^+$ > **3H**$^+$

Consideration of these discrepancies suggests that the use of "rotational" method for calculating the IHB energies of tetrafluoroborates is somewhat questionable. Strictly speaking, the E_{HB} values obtained in these cases characterize not so much the energy of the intramolecular NHN hydrogen bond in the salts as the difference between total energy of bifurcated hydrogen bonds in the close form and energy of the external F…H bond in the corresponding open form. Such an approach would be acceptable providing that the approximate equality of the energies $E_{F...H}$ in the open and closed forms is obtained. However, from Tables S13 and S14 [parameter $R_{F...H}$ (close)/$R_{F...H}$ (open)] it follows that this is far from the case, especially for salt **18H**$^+$**BF**$_4^-$. The relatively satisfactory results when using the "rotational" method for tetrafluoroborates in acetonitrile can be explained by the significant polarity of this solvent, which contributes to the strong separation of ion pairs.[38] In particular, this is evidenced by the considerable increase in the $R_{F...H}$ distance in closed forms of the tetrafluoroborates in MeCN compared to the gas phase (ESI, Tables S13 and S14). In fact, the structure of tetrafluoroborates in acetonitrile can be regarded as approaching that in the "naked" cations. Judging by the sharp increase in the F...H distance this is especially true for salts **18H**$^+$**BF**$_4^-$ and **7H**$^+$**BF**$_4^-$ (Table S13). Notably, that, judging by the X-ray experimental distances F...H (given below in brackets), the IHB strength in salt **18H**$^+$**BF**$_4^-$ also far exceeds that in the benzo[*g*]indole tetrafluoroborates. We believe that the absence of any bifurcation in the solid **18H**$^+$**BF**$_4^-$ mainly results from sterics since the orthogonal to the naphthalene system 8-phenyl group actually acts as a "wall" preventing the approach of the BF_4^- anion to the NH^+ proton (see also Figure 4). Apparently, to a lesser extent this effect should be also manifested in salt **7H**$^+$**BF**$_4^-$.

18H$^+$**BF**$_4^-$ (3.67 Å) > **5H**$^+$**BF**$_4^-$ (2.40 Å) > **4H**$^+$**BF**$_4^-$ (2.25 Å) > **3H**$^+$**BF**$_4^-$ (2.17 Å)

Conclusions

In summary, two types of unique pre-organized model compounds, namely protonated 9-dimethylamino-1-methylbenzo[*g*]indoles **3·HBF$_4$**–**6·HBF$_4$** and 1-dimethylamino-8-(pyrrolyl-1)naphthalene **7·HBF$_4$**, in which a neutral pyrrole nitrogen atom could serve as an *n*- or π-donor at the formation of intramolecular NHN hydrogen bond, were prepared and studied. It has been found that in both cases the NH proton, being strongly shifted to the NMe_2 group, closes the IHB which is centered on the pyrrole N atom. The average energy of such binding lies in the range of 7–10 kcal mol^{-1}, according to the DFT calculated data. This is the first example of such kind of hydrogen bonding in pyrroles; in all previously reported cases, the X–H bond was pointed to annular carbons or ring centroid. At the same time, the principal difference between the two above model systems is that while in the benzoindole cations the pyrrole N atom is markedly pyramidalized, in the **7H**$^+$ cation it remains practically flat. On this basis, IHB in **7H**$^+$ was attributed to the NH...N(π) type since the pyrrole heteroatom actually appears here as a part of the aromatic system, whereas the NHN binding in benzoindole cations seems to be reasonably classified as mixed NH…N(*n*,π) interaction.

Experimental Section

General. If not indicated otherwise, solution ^{1}H and ^{13}C NMR experiments were performed with a 600 MHz spectrometer using the solvent residual peaks as the internal reference. ^{15}N Chemical shifts were referenced relative to nitromethane. All reagents and starting materials were obtained from commercial sources and used without further purification. 9-Dimethylaminobenzo[*g*]indoles **3** and **4** were synthesized as described in ref.[17a] Benzo[*g*]indole **6** was synthesized according to the published procedure[25] while the synthesis of compound **5** was described in ref.[17b]

***N,N*,1-Trimethyl-1*H*-benzo[*g*]indol-9-amine (3).** ^{1}H NMR (CD_3CN, 600 MHz, 30 °C) δ 2.65 (s, 6H), 4.02 (s, 3H), 6.59 (d, J = 3.04 Hz, 1H), 7.14 (dd, J = 7.93, 1.18 Hz, 1H), 7.18 (d, J = 3.04 Hz, 1H), 7.29 (t, J = 7.83 Hz, 1H), 7.40 (d, J = 8.39 Hz, 1H), 7.50 (dd, J = 7.93, 1.18 Hz, 1H), 7.59 (d, J = 8.39 Hz, 1H); ^{13}C{^{1}H} NMR (CD_3CN, 150 MHz, 30 °C) δ 39.4, 42.7, 103.0, 114.1, 118.6, 121.2, 121.3, 122.9, 124.0, 127.2, 131.3, 132.2, 134.0, 148.8.

***N,N*,1,3-Tetramethyl-2-*p*-tolyl-1*H*-benzo[*g*]indol-9-amine (4).** ^{1}H NMR (CD_3CN, 600 MHz, 30 °C) δ 2.36 (s, 3H), 2.43 (s, 3H), 2.76 (s, 6H), 3.61 (s, 3H), 7.13 (dd, J = 7.92, 1.03 Hz, 1H), 7.30 (t, J = 7.84 Hz, 1H), 7.36 (d, J = 8.29 Hz, 2H), 7.45 (d, J = 8.29 Hz, 2H), 7.48 (d, J = 8.41 Hz, 1H), 7.52 (dd, J = 7.92, 1.03 Hz, 1H), 7.63 (d, J = 8.41 Hz, 1H); ^{13}C{^{1}H} NMR (CD_3CN, 150 MHz, 30 °C) δ 9.1, 20.5,

38.5, 42.4, 110.2, 113.9, 118.1, 119.0, 121.3, 122.6, 124.1, 127.4, 129.4, 129.9, 130.6, 134.2, 134.8, 137.7, 140.8, 148.8.

Proton Complexes with Tetrafluoroboric Acid (Hydrogen Tetrafluoroborates) were prepared by mixing equimolar amounts of bases **3**–**6** (usually 0.05 mmol) and 40% aqueous HBF_4 in a minimum volume of EtOAc (1.5 to 2 mL) followed by 3-fold dilution with Et_2O. The residue thus formed was washed with Et_2O (except for **6·HBF$_4$**) and vacuum dried to give the desired salts in high yield. In case of **6·HBF$_4$**, the solvents from clear solution were deleted in vacuum and the non-crystalline residue thus formed was vacuum dried to give **6·HBF$_4$** as clear caramel.

***N*,*N*,1-Trimethyl-1*H*-benzo[*g*]indol-9-amine Hydrogen Tetrafluoroborate (3·HBF$_4$):** 58% (18 mg from 22 mg of **3**); pale-yellow plates with mp 136–138 °C (decomp.). ^{1}H NMR (CD_3CN, 600 MHz, 30 °C): δ 3.39 (br. s, 6H), 3.88 (s, 3H), 6.86 (br. s, 1H), 7.41 (br. s, 1H), 7.61–7.64 (m, 2H), 7.82–7.83 (m, 1H), 7.94–7.95 (m, 1H), 8.13–8.15 (m, 1H), 8.28 (br. s, 1H, NH); ^{13}C{^{1}H} NMR (CD_3CN, 150 MHz, 30 °C) δ 38.0, 50.1, 106.6, 113.6, 118.4, 122.0, 123.0, 124.3, 129.9, 130.1, 131.4, 133.7, 134.9, 135.9. Anal. Calcd for $C_{15}H_{17}BF_4N_2$ (312.12): C, 57.72; H, 5.49; N, 8.98. Found: C, 57.41; H, 5.62; N, 9.07.

***N*,*N*,1,3-Tetramethyl-2-*p*-tolyl-1*H*-benzo[*g*]indol-9-amine Hydrogen Tetrafluoroborate (4·HBF$_4$):** 80% (12 mg from 12 mg of **4**); light-beige prisms with mp 203–205 °C (darken above 175 °C). ^{1}H NMR (CD_3CN, 600 MHz, 30 °C) δ 2.41 (s, 3H), 2.45 (s, 3H), 3.43 (s, 3H), 3.49 (d, J = 4.61 Hz, 6H), 7.42 (d, J = 7.87 Hz, 2H), 7.63–7.67 (m, 3H), 7.77 (d, J = 8.41 Hz, 1H), 7.87 (d, J = 8.41 Hz, 1H), 7.99 (br. d, J = 7.72 Hz, 1H), 8.19 (br. d, J = 7.72 Hz, 1H), 8.42 (br. s, 1H, NH); ^{13}C{^{1}H} NMR (CD_3CN, 150 MHz, 30 °C) δ 9.2, 20.6, 39.1, 50.0, 113.9, 114.3, 118.8, 121.0, 122.8, 124.1, 128.5, 129.6, 130.7, 131.5, 131.7, 133.4, 133.7, 136.0, 138.8, 146.0. Anal. Calcd for $C_{23}H_{25}BF_4N_2$ (416.27): C, 66.36; H, 6.05; N, 6.73. Found: C, 66.52; H, 6.12; N, 6.49.

***N*,*N*,1,3-Tetramethyl-2-*p*-nitrophenyl-1*H*-benzo[*g*]indol-9-amine Hydrogen Tetrafluoroborate (5·HBF$_4$):** 74% (14 mg from 15 mg of **5**); yellow-brown needles with mp 216–217 °C (decomp.). ^{1}H NMR (CD_3CN, 600 MHz, 30 °C) δ 2.49 (s, 3H), 3.46 (s, 3H), 3.52 (br. s, 6H), 7.38–7.44 (m, 1H), 7.68–7.70 (m, 1H), 7.80–7.81 (m, 1H), 7.90–7.91 (m, 1H), 8.02–8.03 (m, 2H), 8.21–8.22 (m, 1H), 8.40–8.41 (br. m, 2H + NH); ^{13}C{^{1}H} NMR (CD_3CN, 150 MHz, 30 °C) δ 9.4, 39.3, 50.2, 113.8, 119.1, 121.2, 123.3, 123.8, 124.0, 124.9, 131.5, 131.8, 132.3, 134.3, 134.7, 136.3, 137.8, 143.6, 147.6. Anal. Calcd for $C_{22}H_{22}BF_4N_3O_2$ (447.24): C, 59.08; H, 4.96; N, 9.40. Found: C, 58.91; H, 5.07; N, 9.43.

***N*,*N*,1-Trimethyl-3-trifluoromethyl-1*H*-benzo[*g*]indol-9-amine Hydrogen Tetrafluoroborate (6·HBF$_4$):** 96% (25 mg from 20 mg of **6**); clear hygroscopic caramel soluble in EtOAc and Et_2O. ^{1}H NMR (CD_3CN, 600 MHz, 30 °C): δ 3.42 (s, 6H), 4.00 (s, 3H), 4.65 (br. s, H_2O + H^+), 7.74 (t, J = 7.95

Hz, 1H), 7.79 (d, *J* = 8.64 Hz, 1H), 7.88 (q, *J* = 1.20 Hz, 1H), 7.90 (dd, *J* = 8.64, 0.88 Hz, 1H), 8.05 (br. d, *J* = 7.96 Hz, 1H), 8.21 (br. d, *J* = 7.96 Hz, 1H); $^{13}C\{^1H\}$ NMR (CD_3CN, 150 MHz, 30 °C) δ 38.4, 50.4, 109.3 (q, *J* = 36.5 Hz), 113.5, 119.7, 120.3, 123.8, 124.5 (q, *J* = 218.3 Hz), 125.6, 130.0, 131.6, 133.4 (q, *J* = 5.0 Hz), 134.0, 139.2, 142.9. Anal. Calcd for $C_{16}H_{16}BF_7N_2$ (380.11): C, 50.56; H, 4.24; N, 7.37. Found: C, 50.42; H, 4.19; N, 7.48.

***N*,*N*-Dimethyl-8-(1*H*-pyrrol-1-yl)naphthalene-1-amine (7).** A mixture of 8-(1*H*-pyrrol-1-yl)naphthalene-1-amine (**16**)[18] (0.208 g, 1.0 mmol), Me_2SO_4 (0.38 mL, 4.0 mmol), $Na_2CO_3 \cdot 10H_2O$ (1.15 g, 4.0 mmol) and MeOH (5 mL) was stirred for 96 h at r.t. The reaction mixture was poured in H_2O (5 mL) and extracted with $CHCl_3$ (3 x 3 mL). Evaporation of the solvent gave 0.198 g (84%) of a mixture of amine **7** and *N*-methyl-8-(1*H*-pyrrol-1-yl)naphthalene-1-amine (**17**). The ratio of compounds **7** and **17** in the mixture based on the ^1H NMR data was 2:1. The mixture was further separated by column chromatography on Al_2O_3 using hexane as eluent. The first fraction with R_f 0.9 gave dimethylaminopyrrole **7** as colorless crystals with mp 50–52 °C. The second fraction with R_f 0.8 allowed to isolate monomethylated amine **17** as colorless solid with mp 54–56 °C. Compound **7:** ^1H NMR (250 MHz, $CDCl_3$) δ 2.42 (s, 6H), 6.23–6.24 (m, 2H), 6.88–6.90 (m, 2H), 7.05 (dd, *J* = 7.4, 1.2 Hz, 1H), 7.38–7.54 (m, 4H), 7.79 (dd, *J* = 7.9, 1.6 Hz, 1H). ^1H NMR (600 MHz, CD_3CN, 30 °C) δ 2.35 (s, 6H), 6.16 (t, *J* = 2.11 Hz, 2H), 6.85 (t, *J* = 2.11 Hz, 2H), 7.07 (d, *J* = 7.51 Hz, 1H), 7.33 (dd, *J* = 7.28, 1.10 Hz, 1H), 7.40 (t, *J* = 7.80 Hz, 1H), 7.44 (t, *J* = 7.72 Hz, 1H), 7.52 (d, *J* = 8.02 Hz, 1H), 7.80 (dd, *J* = 8.15, 0.95 Hz, 1H). ^1H NMR (250 MHz, DMSO-d_6) δ 2.34 (s, 6H), 6.13–6.15 (m, 2H), 6.90–6.92 (m, 2H), 7.08 (dd, *J* = 7.5, 0.9 Hz, 1H), 7.37 (dd, *J* = 7.3, 1.3 Hz, 1H), 7.39–7.54 (m, 2H), 7.58 (dd, *J* = 8.1, 0.9 Hz, 1H), 7.87 (dd, *J* = 8.1, 1.2 Hz, 1H). $^{13}C\{^1H\}$ NMR (150 MHz, CD_3CN, 30 °C) δ 43.2, 107.5, 115.4, 117.4, 122.2, 124.0, 124.8, 125.5, 126.6, 128.1, 137.5, 138.0, 150.0. $^{13}C\{^1H\}$ NMR (62.9 MHz, DMSO-d_6) δ 43.8, 107.8, 115.5, 121.2, 122.3, 124.1, 125.0, 125.9, 126.8, 128.3, 137.3, 137.5, 149.7. Anal. Calcd for $C_{16}H_{16}N_2$ (236.31): C, 81.32; H, 6.82; N, 11.85. Found: C, 81.41; H, 6.93; N, 11.94. ***N*-Methyl-8-(1*H*-pyrrol-1-yl)naphthalene-1-amine (17):** ^1H NMR (250 MHz, DMSO-d_6) δ 2.55 (d, *J* = 4.9 Hz, 3H), 3.48 (br. q, *J* = 4.5 Hz, 1H), 6.35–6.37 (m, 2H), 6.49 (d, *J* = 7.5 Hz, 1H), 6.95–6.96 (m, 2H), 7.21–7.27 (m, 2H), 7.35–7.48 (m, 2H), 7.90 (dd, *J* = 8.2, 1.2 Hz, 1H). $^{13}C\{^1H\}$ NMR (62.9 MHz, DMSO-d_6) δ 31.4, 105.2, 109.9, 116.4, 119.1, 124.2, 125.2, 125.7, 127.8, 130.0, 136.4, 136.5, 145.0. IR (nujol) ν_{max} 3470 cm^{-1}. Anal. Calcd for $C_{15}H_{14}N_2$ (222.28): C, 81.05; H, 6.35; N, 12.60. Found: C, 81.14; H, 6.45; N, 12.70.

***N*,*N*-Dimethyl-8-(1*H*-pyrrol-1-yl)naphthalene-1-amine Hydrogen Tetrafluoroborate (7·HBF$_4$)** was generated on addition of equimolar amount of 48% tetrafluoroboric acid to a solution of compound **7** in CD_3CN in an NMR ampoule. ^1H NMR (600 MHz, CD_3CN, 30 °C) δ 3.17 (d, *J* = 5.12 Hz, 6H),

6.40 (br. s, 1H), 6.66 (t, J = 2.05 Hz, 2H), 7.19 (t, J = 2.05 Hz, 2H), 7.73–7.80 (m, 3H), 7.99 (d, J = 7.83 Hz, 1H), 8.24 (dd, J = 8.09, 1.37 Hz, 1H), 8.27 (d, J = 8.24 Hz, 1H). $^{13}C\{^1H\}$ NMR (150 MHz, CD_3CN, 30 °C) δ 50.1, 113.2, 117.6, 121.9, 123.9, 126.9, 127.2, 130.2, 131.5, 132.4, 133.2, 135.9, 138.1.

Synthesis of *N*,*N*-dimethyl-5-(1*H*-pyrrol-1-yl)naphthalene-1-amine (15) (see ESI, p. S2 for general scheme).

1-(5-Nitronaphthalene-1-yl)-1*H*-pyrrole (B). A mixture of 5-nitronaphthalene-1-amine (**A**) (0.376 g, 2.0 mmol), 2,5-dimethoxytetrahydrofuran (1 mL, 7.6 mmol) and AcOH (10.0 mL) was refluxed for 2 h. The reaction mass was evaporated followed by column chromatography of the residue (Al_2O_3, $CHCl_3$, R_f 0.5) to yield 0.376 g (79%) of the title compound as yellow crystals with mp 102–103 °C (MeOH). ^1H NMR (250 MHz, $CDCl_3$) δ 6.39–6.43 (m, 2H), 6.94–6.98 (m, 2H), 7.53 (dd, J = 8.5, 7.7 Hz, 1H), 7.60 (dd, J = 7.3, 1.0 Hz, 1H), 7.74 (dd, J = 8.8, 7.0 Hz, 1H), 7.96 (d, J = 8.6 Hz, 1H), 8.22 (dd, J = 7.6, 1.0 Hz, 1H), 8.54 (d, J = 8.8 Hz, 1H). $^{13}C\{^1H\}$ NMR (62.9 MHz, $CDCl_3$) δ 109.8, 122.9, 123.5, 124.4, 124.9, 125.2, 126.9, 128.8, 129.8, 131.3, 138.7, 147.1. Calcd for $C_{14}H_{10}N_2O_2$ (238.24): C, 70.58; H, 4.23; N, 11.76. Found: C, 70.65; H, 4.34; N, 11.67.

5-(1*H*-Pyrrole-1-yl)naphthalene-1-amine (C). A mixture of pyrrole **B** (0.357 g, 1.5 mmol), Fe powder (0.504 g, 9.0 mmol), $FeSO_4 \cdot 7H_2O$ (0.081 g, 0.3 mmol) and H_2O (5.0 mL) was refluxed for 3.5 h. Then EtOH (3.0 mL) and charcoal were added to the mixture, boiled for 30 min, filtered and extracted with $CHCl_3$ (3 x 5 mL). The organic fraction was purified by column chromatography on Al_2O_3 (eluent – $CHCl_3$–light petroleum ether, 1:1), collecting a fraction with R_f 0.6. This yielded 0.24 g (77%) of the title compound as a red-brown oil. ^1H NMR (250 MHz, $CDCl_3$) δ 4.21 (br. s, 2H), 6.36–6.40 (m, 2H), 6.81 (dd, J = 7.3, 1.0 Hz, 1H), 6.95–6.99 (m, 2H), 7.15 (d, J = 8.5 Hz, 1H), 7.26–7.30 (m, 1H), 7.40–7.49 (m, 2H), 7.83–7.87 (m, 1H). Anal. Calcd for $C_{14}H_{12}N_2$ (208.26): C, 80.74; H, 5.81; N, 13.45. Found: C, 80.67; H, 5.90; N, 13.36.

***N*,*N*-Dimethyl-5-(1*H*-pyrrol-1-yl)naphthalene-1-amine (15).** A mixture of amine **C** (0.208 g, 1.0 mmol), Me_2SO_4 (0.38 mL, 4.0 mmol), $Na_2CO_3 \cdot 10H_2O$ (1.15 g, 4.0 mmol) and MeOH (5 mL) was stirred for 96 h at rt. The reaction mixture was poured in H_2O (5 mL) and extracted with $CHCl_3$ (3 x 3 mL). Column chromatography of the residue (Al_2O_3, $CHCl_3$, R_f 0.9) yielded 0.179 g (76%) of the title compound as light brown oil. ^1H NMR (250 MHz, $CDCl_3$) δ 2.92 (s, 6H), 6.38–6.40 (m, 2H), 6.97–6.98 (m, 2H), 7.09–7.13 (m, 1H), 7.36–7.53 (m, 4H), 8.29 (dd, J = 8.2, 1.1 Hz, 1H). $^{13}C\{^1H\}$ NMR (62.9 MHz, $CDCl_3$) δ 45.3, 108.8, 114.6, 118.0, 123.3, 123.4, 124.2, 124.4, 126.8, 129.8, 131.5, 138.6, 151.0. EI MS *m*/*z* (%): 236 (23) $[M]^+$, 221 (5) $[M - Me]^+$, 205 (17) $[M - 2Me - H]^+$, 97 (41), 85 (42),

57 (100). Anal. Calcd for $C_{16}H_{16}N_2$ (236.31): C, 81.32; H, 6.82; N, 11.85. Found: C, 81.35; H, 6.83; N, 11.82.

***N*,*N*-Dimethyl-5-(1*H*-pyrrol-1-yl)naphthalene-1-ammonium Picrate (15H$^+$PicO$^-$).** A solution of dimethylaminopyrrole **15** (28 mg, 0.12 mmol) in EtOH (1 mL) was added to a solution of PicOH (33 mg, 0.12 mmol) in EtOH (1 mL). The mixture was kept at –10 °C for 1 h, the precipitate thus formed was filtered off and washed with cold Et_2O (1 mL). Yield 50 mg (90%). Yellow-green crystals with mp 107–108 °C (decomp.). ^{1}H NMR (250 MHz, $CDCl_3$, 21 °C) δ 3.40 (s, 6H), 6.40–6.41 (m, 2H), 6.94–6.96 (m, 2H), 7.49–7.64 (m, 4H), 7.77 (d, J = 7.9 Hz, 1H), 8.37 (d, J = 8.3 Hz, 1H), 8.99 (s, 2H). ^{1}H NMR (250 MHz, $CDCl_3$, –56 °C) δ 3.54 (s, 6H), 6.42 (br. s, 2H), 6.98 (br. s, 2H), 7.55–7.63 (m, 3H), 7.75 (d, J = 7.2 Hz, 1H), 7.92 (d, J = 8.3 Hz, 1H), 8.31 (d, J = 7.9 Hz, 1H), 9.04 (s, 2H), 13.19 (s, 1H). ^{1}H NMR (250 MHz, DMSO-d_6, 50 °C) δ 3.00 (s, 6H), 6.28–6.30 (m, 2H), 6.99–7.01 (m, 2H), 7.33 (d, J = 8.2 Hz, 1H), 7.62 (dd, J = 8.5, 7.3 Hz, 1H), 8.23 (d, J = 8.5 Hz, 1H), 8.53 (s, 2H). Anal. Calcd for $C_{22}H_{19}N_5O_7$ (465.41): C, 56.77; H, 4.11; N, 15.05. Found: C, 56.87; H, 4.20; N, 15.13.

***N*,*N*-Dimethyl-8-phenylnaphthalene-1-amine (18).** A mixture of 8-phenylnaphthalene-1-amine[39] (0.1 g, 0.46 mmol), Me_2SO_4 (1.5 mL, 15.83 mmol), $Na_2CO_3 \cdot 10H_2O$ (1.31 g, 4.58 mmol) and H_2O (0.5 mL) was stirred for 24 h at rt. Next, the reaction mass was poured in H_2O (5 mL), extracted with CH_2Cl_2 (3 x 3 mL), evaporated to dryness and subjected to column chromatography (Al_2O_3, CH_2Cl_2, R_f 0.9) to obtain 0.058 g (51%) of the title compound as yellow-brown oil. ^{1}H NMR (250 MHz, $CDCl_3$) δ 2.24 (s, 6H), 7.06 (d, J = 7.4 Hz, 1H), 7.27–7.49 (m, 8H), 7.57 (d, J = 8.0 Hz, 1H), 7.80 (dd, J = 8.0, 1.1 Hz, 1H). ^{1}H NMR (250 MHz, CD_3CN) δ 2.22 (d, J = 0.8 Hz, 6H), 7.13 (d, J = 7.4 Hz, 1H), 7.29–7.38 (m, 6H), 7.45 (dd, J = 7.3, 4.4 Hz, 1H), 7.54 (dd, J = 9.3, 2.2 Hz, 1H), 7.61 (d, J = 8.1 Hz, 1H) 7.86 (d, J = 8.1 Hz, 1H). ^{1}H NMR (250 MHz, DMSO-d_6) δ 2.17 (s, 6H), 7.09 (dd, J = 7.4, 1.0 Hz, 1H), 7.27–7.32 (m, 6H), 7.42–7.52 (m, 2H), 7.61 (dd, J = 8.1, 0.9 Hz, 1H), 7.86 (dd, J = 8.1, 1.2 Hz, 1H). ^{13}C{^{1}H} NMR (62.9 MHz, $CDCl_3$) δ 43.5, 115.6, 123.1, 125.0, 125.6, 125.7, 126.0, 128.2, 129.2, 129.7, 136.5, 139.7, 144.2, 150.9. EI MS m/z (%): 247 (99) $[M]^+$, 232 (10) $[M - CH_3]^+$, 217 (17) $[M - 2CH_3]^+$. Anal. Calcd for $C_{18}H_{17}N$ (247.33): C, 87.41; H, 6.93; N, 5.66. Found: C, 87.49; H, 6.84; N, 5.73.

***N*,*N*-Dimethyl-8-phenylnaphthalene-1-amine Hydrogen Tetrafluoroborate (18·HBF$_4$)** was obtained by a procedure analogous to the synthesis of protic complexes **3·HBF$_4$**–**5·HBF$_4$**. Yield 40% (15 mg from 28 mg of **18**); colorless crystals with mp 131–132 °C. ^{1}H NMR (600 MHz, CD_3CN, 30 °C) δ 3.02 (d, J = 5.28 Hz, 6H), 7.52 (dd, J = 7.07, 1.09 Hz, 1H), 7.66–7.68 (m, 2H), 7.72–7.76 (m, 5H), 7.89 (d, J = 7.57 Hz, 1H), 8.09 (br. s, 1H), 8.15 (dd, J = 8.28, 0.85 Hz, 1H), 8.23 (d, J = 8.12 Hz, 1H). Anal. Calcd for $C_{18}H_{18}BF_4N$ (335.15): C, 64.51; H, 5.41; N, 4.18. Found: C, 64.60; H, 5.48; N, 4.27.

Supporting Information

Electronic supplementary information (ESI) available: X-ray crystallographic data, spectral data, additional comments and computational details (PDF). Atomic coordinate file of all calculated structures (XYZ). CCDC 1837903–1837905 and 1867330–1867332. For ESI and crystallographic data in CIF or other electronic format see DOI: ...

Acknowledgements

This work was supported by the Russian Foundation for Basic Research (Project No. 17-03-00035). X-ray studies were performed by Dr. Kyrill Y. Suponitsky (A. N. Nesmeyanov Institute of Organoelement Compounds, Russian Academy of Sciences, Moscow). We acknowledge the Wrocław Centre for Networking and Supercomputing (WCSS) for generous grants of computer time.

References and Notes

(1) Pauling, L.; Pauling, P. *Chemistry*; Freeman, W. H. & Co.: San Francisco, 1975, 792 p.

(2) (a) Steiner, T.; Koellner, G. Hydrogen bonds with π-acceptors in proteins: frequencies and role in stabilizing local 3D structures. *J. Mol. Biol*. **2001**, *305*, 535–557. (b) Fernandez-Recio, J.; Romero, A.; Sancho, J. Energetics of a hydrogen bond (charged and neutral) and of a cation-π interaction in apoflavodoxin. *J. Mol. Biol*. **1999**, *290*, 319–330.

(3) Ma, J. C.; Dougherty, D. A. The Cation−π Interaction. *Chem. Rev*. **1997**, *97*, 1303–1324.

(4) Mahadevi, A. S.; Sastry, G. N. Cation−π Interaction: Its Role and Relevance in Chemistry, Biology, and Material Science. *Chem. Rev*. **2013**, *113*, 2100–2138.

(5) (a) Zhang, R. B.; Somers, K. R. F.; Kryachko, E. S.; Nguen, M. T.; Zeegers-Huyskens, T.; Ceulemans, A. Hydrogen Bonding to π-Systems of Indole and 1-Methylindole: Is There Any OH···Phenyl Bond? *J. Phys. Chem. A* **2005**, *109*, 8028–8034. (b) Muñoz, M. A.; Galán, M.; Gómez, I.; Carmona, C.; Guardado, P.; Balón, M. The pyrrole ring as hydrogen-bonding π-donor base: an experimental and theoretical study of the interactions of *N*-methylpyrrole with alcohols. *Chem. Phys*. **2003**, *290*, 69–77.

(6) (a) Goddard, R.; Heinemann, O.; Krüger, C. Pyrrole and a Co-crystal of 1*H*- and 2*H*-1,2,3-Triazole. *Acta Cryst*. **1997**, *C53*, 1846–1850. (b) Stefov, V.; Pejov, L.; Šoptrajanov, B. Experimental and quantum chemical study of pyrrole self-association through N–H···π hydrogen bonding. *J. Mol. Struct*. **2003**, *649*, 231–243.

(7) Evans, D. A.; Borg, G.; Scheidt, K. A. Remarkably Stable Tetrahedral Intermediates: Carbinols from Nucleophilic Additions to *N*–Acylpyrroles. *Angew. Chem. Int. Ed*. **2002**, *41*, 3188–3191.

(8) Katritzky, A. R.; Pozharskii, A. F. *Handbook of Heterocyclic Chemistry*; 2nd ed.; Pergamon: Amsterdam, 2000, p. 58.

(9) There is a single communication on protonation of pyrrole nitrogen atom in solution.[10] Thus, on treatment of carbazole and *N*-methylcarbazole with fluorosulphuric acid at 30 °C cations **A** and **B** were registered by ^{1}H NMR spectroscopy. Their pK_a values were estimated as equal to –6.0 and –8.0, respectively. Indole and *N*-methylindole are protonated exclusively at the C-3 atom with pK_a –3.5 and –2.32, respectively,[11] while the protonation of pyrrole in solution occurs kinetically at the β-position with fast rearrangement of the primarily formed C_β adduct into more stable C_α. For pyrrole and 1-methylpyrrole, pK_a's of –3.80 and –2.90 were reported.[12] For the protonation of pyrrole and indole at the nitrogen atom, extrapolation value of pK_a about –10 was suggested.[10] Accordingly to Speranza, pyrrole in the gas phase is tritiated with the $^3He^3H^+$ electrophilic reagent at the N, C_α and C_β positions with the ratio 18, 37 and 45%, respectively.[13] However, theoretical calculations of the gas-phase protonation energies showed that the α-protonation of pyrrole (PA = 208.9 kcal mol^{-1}) is more preferable than β (205.2 kcal mol^{-1}).[14]

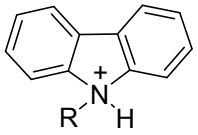

A (R = H)
B (R = Me)

(10) Chen, H. J.; Hakka, L. E.; Hinman, R. L.; Kresge, A. J.; Whipple, E. B. Basic strength of carbazole. Estimate of the nitrogen basicity of pyrrole and indole. *J. Am. Chem. Soc*. **1971**, *93*, 5102–5107.

(11) *Indoles*; ed. Houlihan, W. J.; Wiley-Intersc.: New York, 1972, part 1, 587 pp.

(12) Jones, R. A.; Bean, J. P. *The Chemistry of Pyrroles*; Academic Press: New York, 1977, 526 pp.

(13) (a) Speranza, M. First example of predominant β-orientation in electrophilic substitution of pyrrole. *Chem. Commun*. **1981**, 1177–1178. (b) Angelini, G.; Lagazzi, G.; Sparapani, C.; Speranza, M. Gas-phase heteroaromatic substitutions. 5. Gas-phase protonation of five-membered heteroaromatic rings by hydro-t-helium(1+)-^{3}He ($^3HeT^+$) ions. A model reaction for a theoretical approach to heteroaromatic reactivity. *J. Am. Chem. Soc*. **1984**, *106*, 37–41. (c) Speranza, M. Gas-phase reactivity of five-membered heteroaromatics toward electrophiles, an experimental check on theoretical predictions. *Pure & Appl. Chem*. **1991**, *63*, 243–254.

(14) Catalan, J.; Yanez, M. The α vs. β protonation of pyrrole and indole. *J. Am. Chem. Soc.* **1984**, *106*, 421–422.

(15) (a) Kirby, A. J.; O'Carroll, F. Highly efficient intramolecular general acid catalysis of enol ether hydrolysis, with rapid proton transfer to carbon. *J. Chem. Soc, Perkin Trans. 2* **1994**, 649–655. (b) Kirby, A. J.; Dutta-Roy, N.; da Silva, D.; Goodman, J. M.; Lima, M. F.; Roussev, C. D.; Nome, F. Intramolecular General Acid Catalysis of Phosphate Transfer. Nucleophilic Attack by Oxyanions on the PO_3^{2-} Group. *J. Am. Chem. Soc.* **2005**, *127*, 7033–7040. (c) Perrin, C. L.; Ohta, B. K. Symmetry of NHN hydrogen bonds in solution. *J. Mol. Struct.* **2003**, *644*, 1–12.

(16) Cox, C.; Wack, H.; Lectka, T. Strong Hydrogen Bonding to the Amide Nitrogen Atom in an "Amide Proton Sponge": Consequences for Structure and Reactivity. *Angew. Chem. Int. Ed*. **1999**, *38*, 798–800.

(17) (a) Filatova, E. A.; Pozharskii, A. F.; Gulevskaya, A. V.; Ozeryanskii, V. A. Multiple transformations of 2-alkynyl-1,8-bis(dimethylamino)naphthalenes into benzo[*g*]indoles. Pd/Cu-Dependent switching of the electrophilic and nucleophilic sites in acetylenic bond and a puzzle of porcelain catalysis. *J. Org. Chem*. **2015**, *80*, 872–881. (b) Filatova, E. A.; Gulevskaya, A. V.; Pozharskii, A. F. Synthesis of 2-aryl-3-methylbenzo[*g*]indoles from 2-(arylethynyl)-1,8-bis(dimethylamino)naphthalenes: new examples of [1,3]-migration involving *N*-methyl group. *Chem. Heterocycl. Compd.* **2018**, *54*, 38–42.

(18) Cheeseman, G. W. H.; Eccleshall, S. A. Synthesis of Pyrrolo[1,2-*a*]naphtho[1,8-*ef*][1,4]diazepines. *J. Heterocyclic Chem.* **1986**, *23*, 65–67.

(19) Alabugin, I. V.; Bresch, S.; Gomes, G. P. Orbital hybridization: a key electronic factor in control of structure and reactivity. *J. Phys. Org. Chem.* **2015**, *28*, 147–162.

(20) Alabugin, I. V.; Manoharan, M.; Buck, M.; Clark, R. J. Substituted anilines: The tug-of-war between pyramidalization and resonance inside and outside of crystal cavities. *J. Mol. Struct. THEOCHEM* **2007**, *813*, 21–27.

(21) Howard, S. T. Relationship between Basicity, Strain, and Intramolecular Hydrogen-Bond Energy in Proton Sponges. *J. Am. Chem. Soc.* **2000**, *122*, 8238–8244.

(22) Pozharskii, A. F.; Ozeryanskii, V. A. in *The Chemistry of Anilines*, ed. Rappoport, Z.; J. Wiley & Sons: Chichester, 2007, Part 2, Ch. 17, pp. 931–1026.

(23) Ozeryanskii, V. A.; Shevchuk, D. A.; Pozharskii, A. F.; Kazheva, O. N.; Chekhlov, A. N.; Dyachenko, O. A. Protonation of naphthalene proton sponges containing higher *N*-alkyl groups. Structural consequences on proton accepting properties and intramolecular hydrogen bonding. *J. Mol. Struct.* **2008**, *892*, 63–67.

(24) Although we do not yet have the X-ray data for **3**, one can assume that configuration of the pyrrole N atom in it should be strongly flatten. A weighty, albeit indirect proof of this suggestion is the earlier reported X-ray data for related compound **9** (Scheme 2) in which the pyrrole ring is nearly planar [ΣN(1) = 358.7°, ΔMe = 0.266 Å].[25]

(25) Kachalkina, S. G.; Borodkin, G. S.; Pozharskii, A. F.; Antonov, A. S.; Borodkina, I. G.; Maltsev, Y. F.; Filatova, E. A.; Filarowski, A.; Ozeryanskii, V. A. Base-promoted transformation of 2-C(O)R-1,8-bis(dimethylamino)naphthalenes into benzo[*g*]indole derivatives. *Mendeleev Commun*. **2015**, *25*, 182–184.

(26) Pozharskii, A. F.; Ozeryanskii, V. A.; Mikshiev, V. Y.; Antonov, A. S.; Chernyshev, A. V.; Metelitsa, A. V.; Borodkin, G. S.; Fedik, N. S.; Dyablo, O. V. 10-Dimethylamino derivatives of benzo[*h*]quinoline and benzo[*h*]quinazolines: fluorescent proton sponge analogues with opposed *peri*-NMe_2/–N= groups. How to distinguish between proton sponges and pseudo-proton sponges. *J. Org. Chem*. **2016**, *81*, 5574–5587.

(27) Notably, the hydrogen bond bifurcation in salt $\mathbf{3H^+BF_4^-}$ significantly exceeds that in $\mathbf{4H^+BF_4^-}$ and $\mathbf{5H^+BF_4^-}$. Probably in the last two salts an approach of BF_4^- to the NH proton is sterically hampered by the 2-aryl groups. This may be an additional factor weakening the IHB in $\mathbf{3H^+BF_4^-}$.

(28) Staab, H. A.; Diehm, M.; Krieger, C. Synthesis, structure and 'proton sponge' properties of 1,12-bis(dimethylamino)benzo[*c*]phenanthrene. *Tetrahedron Lett.* **1995**, *36*, 2967–2970.

(29) Kaljurand, I.; Kütt, A.; Sooväli, L.; Rodima, T.; Mäemets, V.; Leito, I.; Koppel, I. A. Extension of the Self-Consistent Spectrophotometric Basicity Scale in Acetonitrile to a Full Span of 28 pK_a Units: Unification of Different Basicity Scales. *J. Org. Chem.* **2005**, *70*, 1019–1028.

(30) Kurasov, L. A.; Pozharskii, A. F.; Kuz'menko, V. V.; Klyuev, N. A.; Chernyshev, A. I.; Goryaev, S. S.; Chikina, N. L. Nitration of 1,8-bis(dialkylamino)naphthalenes. *Zh. Org. Khim.* **1983**, *19*, 590–597.

(31) Problems arising during growing crystals of salt $\mathbf{7H^+BF_4^-}$ are caused by its tendency to transform into another compound; unusual chemistry of this conversion will be reported soon.

(32) Burov, O. N.; Kletskii, M. E.; Fedik, N. S.; Kurbatov, S. V.; Lisovin, A. V. Experimental and quantum-chemical study of nucleophilic substitution mechanism in berberine. *Chem. Heterocycl. Compd.* **2015**, *51*, 997–1007.

(33) It is noteworthy, that similar scale of theoretically E_{HB} values (10–22 kcal mol^{-1}) was reported for the $NH^+\ldots\pi$ complexes of benzene and ethylene with NH_4^+, $Me_2NH_2^+$ and $MeNH_3^+$ ions: (a) Lee, J. Y.; Lee, S. J.; Choi, H. S.; Cho, S. J.; Kim, K. S.; Ha, T.-K. Ab initio study of the complexation of benzene with ammonium cations. *Chem. Phys. Lett*. **1995**, *232*, 67–71. (b) Deakyne, C. A.; Meot-

Ner (Mautner) M. Unconventional ionic hydrogen bonds. 2. $NH^{+}\cdots\pi$ Complexes of onium ions with olefins and benzene derivatives. *J. Am. Chem. Soc*. **1985**, *107*, 474–479.

(34) (a) Reed, A. E.; Weinhold, F.; Curtiss, L. A.; Pochatko, D. J. Natural bond orbital analysis of molecular interactions: Theoretical studies of binary complexes of HF, H_2O, NH_3, N_2, O_2, F_2, CO, and CO_2 with HF, H_2O, and NH_3. *J. Chem. Phys.* **1986**, *84*, 5687–5705. (b) Stone, A. J. Natural Bond Orbitals and the Nature of the Hydrogen Bond. *J. Phys. Chem. A*. **2017**, *121*, 1531–1534.

(35) (a) Arunan, E.; Desiraju, G. R.; Klein, R. A.; Sadlej, J.; Scheiner, S.; Alkorta, I.; Clary, D. C.; Crabtree, R. H.; Dannenberg, J. J.; Hobza, P.; Kjaergaard, H. G.; Legon, A. C.; Mennucci, B.; Nesbitt, D. J. *Definition of the hydrogen bond* (IUPAC Recommendations, 2011), *Pure App. Chem*. **2011**, *83*, 1637–1641. (b) Parthasarathi, R.; Subramanian, V. in *Hydrogen Bonding – New Insights*; ed. Grabowski, S.; Springer, 2006, pp. 1–50.

(36) (a) Perrin, C. L.; Ohta, B. K. Symmetry of N−H−N Hydrogen Bonds in 1,8-Bis(dimethylamino)naphthalene·H^{+} and 2,7-Dimethoxy-1,8-bis(dimethylamino)naphthalene·H^{+}. *J. Am. Chem. Soc*. **2001**, *123*, 6520–6526. (b) Anslyn, E. V.; Dougherty, D. A. *Modern Physical Organic Chemistry*; University Science Books: Sausalito, CA, 2006, p 179. (c) Llamas-Saiz, A. L.; Foces-Foces, C.; Elguero, J. Proton sponges. *J. Mol. Struct*. **1994**, *328*, 297–323. (d) Pozharskii, A. F.; Ozeryanskii, V. A. Proton sponges and hydrogen transfer phenomena. *Mendeleev Commun*. **2012**, *22*, 117–124.

(37) Degtyarev, A. V.; Ryabtsova, O. V.; Pozharskii, A. F.; Ozeryanskii, V. A.; Starikova, Z. A.; Sobczyk, L.; Filarowski, A. 2,7-Disubstituted proton sponges as borderline systems for investigating barrier-free intramolecular hydrogen bonds. Protonated 2,7-bis(trimethylsilyl)- and 2,7-di(hydroxymethyl)-1,8-bis(dimethylamino)naphthalenes. *Tetrahedron* **2008**, *64*, 6209–6214.

(38) Kütt, A.; Leito, I.; Kaljurand, I.; Sooväli, L.; Vlasov, V. M.; Yagupolskii, L. M.; Koppel, I. A. A Comprehensive Self-Consistent Spectrophotometric Acidity Scale of Neutral Brønsted Acids in Acetonitrile. *J. Org. Chem.* **2006**, *71*, 2829–2838.

(39) Jurok, R.; Cibulka, R.; Dvořáková, H.; Hampl, F.; Hodačová, J. Planar Chiral Flavinium Salts – Prospective Catalysts for Enantioselective Sulfoxidation Reactions. *Eur. J. Org. Chem*. **2010**, 5217–5224.